

## Kinetic-energy functional of the electron density

Lin-Wang Wang

*Laboratory of Atomic and Solid State Physics, Cornell University, Ithaca, New York 14853*

Michael P. Teter

*Applied Process Research, Corning Inc., Ithaca, New York 14853*

*and Laboratory of Atomic and Solid State Physics, Cornell University, Ithaca, New York 14853*

(Received 5 September 1991; revised manuscript received 3 February 1992)

A kinetic-energy functional of the electronic density is presented. This functional is based on an integral form and is correct through second order in the response. The formulas are compared numerically with the Thomas–Fermi–von Weizsäcker–like formulas and favorable results are found. These formulas correctly give both shell structures in the electron densities of atoms and bond charges in the electron densities of solids. This quantum oscillation in the electron density is lacking in the densities of previous kinetic-energy functionals and is regarded as the major achievement of the current approach.

### I. INTRODUCTION

Considerable effort has been expended to create an approximate kinetic-energy functional of the electron density which is accurate enough to model chemistry but simple enough for fast computation.<sup>1</sup> If our goal is to simulate a large group of atoms in dynamic motion, the Kohn-Sham functional used in the local-density approximation becomes unwieldy as the number of atoms approaches 100. An accurate and computationally inexpensive kinetic-energy density functional is highly desirable in the simulation of condensed-matter systems, because, in that environment, the solution of the Kohn-Sham equation for a large number of bands and  $\mathbf{k}$  points can be reduced to the calculation of a single function by using the kinetic-energy functional.

Throughout this paper, the kinetic energy is the noninteracting Fermion kinetic energy, which is defined as

$$T[n] = \min \left\langle \Psi \left| \left[ -\frac{1}{2} \sum_i \nabla_i^2 \right] \right| \Psi \right\rangle \quad (1.1)$$

for all  $\Psi$ 's that yield  $n$ . Here  $\Psi$  is the total wave function, and  $n$  is the total electron density. The  $\Psi$  which gives the minimum kinetic energy is a product of single-particle wave functions. This kinetic energy is the same kinetic energy used in the Kohn-Sham equations. In all the numerical comparisons, therefore, we will compare our results to the Kohn-Sham equation results.

The first successful approximation to a kinetic-energy functional was the Thomas-Fermi (TF) formula.<sup>2</sup> It has several shortcomings. The electron density at an atomic nucleus is infinite, and its tail decays as an inverse power law. Teller was able to prove that there was no stable chemical binding with the TF formula.<sup>3</sup> One way to improve the TF formula is the generalized Thomas–Fermi–von Weizsäcker (TF $\lambda$ W) formula, which adds  $\lambda$  times a gradient term to the TF theory. It has the form

$$T[n] = \frac{3}{10} (3\pi^2)^{2/3} \int n^{5/3}(r) d^3r - \lambda \frac{1}{2} \int n^{1/2}(r) \nabla^2 n^{1/2}(r) d^3r, \quad (1.2)$$

where  $\lambda$  is an adjustable parameter. This addition corrects the nuclear and tail problems and leads to stable binding of atoms. For  $\lambda=1$ , we have the original Thomas–Fermi–von Weizsäcker formula.<sup>4</sup> The combination of both the TF term and the full von Weizsäcker term gives a rigorous upper limit to the kinetic energy. Thus, the kinetic energy of this combination is usually much too high. It was later determined that  $\lambda=\frac{1}{9}$  is the proper coefficient for the second-order formula of the gradient expansion theory.<sup>5</sup> Computational experience seems to show that  $\lambda=\frac{1}{5}$  (Ref. 6) gives the best results of all the possible values of  $\lambda$  when used to calculate the kinetic energy of atoms from Hartree-Fock densities. For Hartree-Fock densities, it is possible to do slightly better using higher-order terms in the gradient expansion. If an electron density is calculated by minimizing the total energy of the electrons, the result is known as a variational density. For variational densities,  $\lambda=\frac{1}{5}$  has been found to give the best results among the TF $\lambda$ W formulas. Again, the gradient expansion can give good results when carried to higher order, but after the fourth order it becomes unstable. The fourth-order result is better than the  $\lambda=\frac{1}{9}$  result, but no better than the  $\lambda=\frac{1}{5}$  result.<sup>7</sup> Because it is simple and leads to almost the best results among the existing kinetic-energy functionals for variational densities, we will use the TF $\lambda$ W formula (especially  $\lambda=\frac{1}{5}$ ) as a representation of the existing formulas in all comparisons in this paper. As mentioned above, the gradient expansion is a more systematic method for improving the Thomas-Fermi formula to higher orders, but above fourth order, the variational calculation becomes unstable. There have been many successes for the gradient expansion theory and its related formulas over the

last two decades. They give very accurate kinetic energies for atoms when the exact densities are used, but there are also serious problems with these formulas. First, they do not treat the tail regions of the atomic densities properly. The gradient expansion series is divergent after fourth order in the tail region. The high accuracy for the kinetic energy is preserved by the fact that the tail region contributes very little total kinetic energy. The tail regions of atoms are extremely important for chemistry, however. A related fact is that, in molecules, for the chemical binding energy, even when the exact Hartree-Fock densities are used, the results are not good.<sup>8</sup> This is caused either by significant residual error left in the higher-order terms in the gradient expansion series, or by the qualitative incorrectness of the formulas in the bonding region.

Use of the above kinetic-energy formulas to calculate the electron densities of atoms and molecules by the variational principle leads to unsatisfactory results.<sup>8</sup> There is no shell structure in the densities. As a result, the chemistry will not be correct (there will be no Periodic Table and its corresponding chemical order characterized by the deviation from filled shells). In the solid, this corresponds to the lack of bond charge in the variational densities of covalent materials, or a lack of charge transfer in ionic materials. This lack of shell structure, bonds, and oscillatory phenomena in general, which has its roots in the quantized nature of the orbitals under study (referred to as quantum-interference effect in the following), remains one of the main challenges for kinetic-energy density functionals.

We would like to make a plausibility argument that the variational density of an atom or molecule will not have an oscillating shell structure for the gradient expansion theory nor will any other kinetic-energy functional which expresses the kinetic-energy density  $t[n]$  as a simple local function of  $n(r)$  and its derivatives. An expansion in derivatives of the kinetic-energy operator is equivalent to a power-series expansion in its Fourier transform. It is well known that the gradient expansion is a series expansion around  $k=0$ , where  $k$  is the wave vector of an oscillation in the density. For any electronic system, the dielectric-response function and the kinetic-energy operator are closely related. It is also well known that the Lindhard response function of the homogeneous electron gas has a derivative discontinuity at  $2k_F$ , and no power series can extrapolate across this discontinuity. At the same time, it is well known that this singularity in the response function gives rise to the quantum oscillations in the density known as Friedel oscillations. In an atom, the variations in density which make up the shells are small, and the corresponding total potential gives almost no hint of an oscillating structure. In the absence of an oscillation in the driving potential, it must be that the addition of the oscillation to the density lowers the total energy in the full quantum-mechanical solution to the atom. If we take the gradient expansion of the kinetic energy through fourth order, and solve for the density variationally, there is no oscillatory structure. Since the solution by definition is the minimum-energy solution for this kinetic-energy operator, the addition of a small oscillato-

ry component to this density must raise the energy.

After considering the various problems and the ways to introduce the quantum oscillations and shell structure, we proposed an integral form for  $t[n]$ , i.e.,

$$t[n](r) = \int f(r, r') n(r') d^3r', \quad (1.3)$$

as the most primitive form. Because  $t[n](r)$  depends on its neighboring density directly through an integral, an oscillating form of  $f(r, r')$  can cause an oscillating variational density. If  $f(r, r')$  is a local function around  $r$ , then  $t[n](r)$  depends only on  $n(r')$  around  $r$ . The formulas following this direction are to be discussed in the following sections. This approach is similar in spirit to the classical weighted-density-functional theory of liquids, especially in their construction of the weighting function to yield the correct free energy through second order.<sup>9</sup>

We would like to discuss some other approaches to kinetic-energy functionals. As outlined above, our approach is an integral formula. Similar approaches existed as early as 1964 when Hohenberg and Kohn<sup>10</sup> presented their density-functional theory. They proposed a series expansion based on the density variation  $n(r) - n_0$ . But the direct application of that form in solids to the linear-response term has not given good results, because the density variation in a solid is usually too large for the linear term to be valid. And the higher-order terms are not easy to compute. They also came up with a partial summation result of a gradient expansion series, but that formula was not studied numerically in that paper. Besides, because the kinetic energy was treated together with the exchange and correlation energy in their approach, it was difficult to get the correct coefficients in the formula. The same line of thought was carried out further by Plumer and Geldart.<sup>11</sup> However, the fact that they used their formula for atoms made them conclude that the approach is unfavorable compared to the gradient expansion theory. While the basic direction is parallel, our formula differs from the previous work by using a different form which fortuitously allows its use over wider density variations. We also carried it through to higher order. We also show how to compute the higher-order response economically. We also emphasize our applications in solid systems with the aid of pseudopotentials. That is the area where the kinetic-energy functionals are most needed and is also the area in which our formula works best. Another interesting approach is that of Herring and Herring and Chopra.<sup>12</sup> The electron density computed from their formula showed some quantum-interference effects for one-dimensional systems. Unfortunately, the application of their formula to three dimensions is very difficult.

## II. FIRST-ORDER KINETIC-ENERGY INTEGRAL FORMULA

Starting with the assumption that the kinetic-energy density at one position is dependent on the density near that point, the simplest form which can represent this local dependence is an integral as discussed above:

$$t[n](r) = \int f(r, r') n(r') d^3r', \quad (2.1)$$

where  $t[n](r)$  is the kinetic-energy density at the three-dimensional point  $r$  and  $f(r, r')$  is to be determined. Thus the total kinetic energy  $E_{\text{kin}}$  can be written as

$$E_{\text{kin}} = \int \int n(r) f(r, r') n(r') d^3r d^3r'. \quad (2.2)$$

However, the TF formula should be the obvious limit of a slowly varying density, thus it is efficacious to change the above formula to

$$E_{\text{kin}} = \int \int n^{5/6}(r) f(r, r') n^{5/6}(r') d^3r d^3r'. \quad (2.3)$$

Based on the above assumption,  $f(r, r')$  must integrate to  $\frac{3}{10}(3\pi^2)^{2/3}$  in order that the above formula will reduce to the TF formula when the typical length of variation of density  $n(r)$  is larger than the range of  $f(r, r')$ . The hope is that the shape or perhaps an oscillatory behavior of  $f(r, r')$  will establish the proper density oscillations which reflect the quantum-mechanical nature of the system.

To simplify the analysis,  $f(r, r')$  is approximated as  $f(k_F|r-r'|)$ , where  $k_F$  is the Fermi momentum for the average density  $n_0$  of the system. The justification for this approximation lies in the fact that the second-order perturbation expansion for the energy is of this form. After this step, the exact form of  $f$  can be obtained from linear-response theory. Suppose there is a small  $\Delta v(r)$ , from the linear-response theory, we can get the perturbation of the density as

$$\Delta n(r) = - \int g(r-r') \Delta v(r') dr', \quad (2.4)$$

or in  $k$  space

$$\Delta N(k) = -G(k) \Delta V(k) \equiv -\frac{k_F}{\pi^2} \mathcal{W} \left[ \frac{k}{k_F} \right] \Delta V(k), \quad (2.5)$$

where

$$\mathcal{W}(q) = \left[ \frac{1}{2} + \frac{(q^2-4)}{8q} \ln \left| \frac{2-q}{2+q} \right| \right], \quad (2.6)$$

and  $q = k/k_F$ . We can also get the perturbation density by using the kinetic-energy functional (2.3). To do that, simply minimize the total noninteracting energy:

$$E_{\text{tot}} = \int \int n^{5/6}(r) f(r, r') n^{5/6}(r') d^3r d^3r' + \int v(r) n(r) d^3r - E_f \int n(r) d^3r, \quad (2.7)$$

where  $E_f$  is the Lagrange multiplier to keep the total number of electrons fixed while making the minimization; physically, it is the chemical potential. Taking the functional derivative of  $E_{\text{tot}}$  and setting it to zero, we get

$$\frac{5}{3} n^{-1/6}(r) \int f(r-r') n^{5/6}(r') d^3r' + v(r) - E_f = 0. \quad (2.8)$$

Now, assuming the perturbation form from the uniform density, i.e.,  $n(r) = n_0 + \Delta n(r)$  and  $v(r) = \Delta v(r)$ , expanding Eq. (2.8) to first order, we have

$$\begin{aligned} \frac{5}{3} n_0^{2/3} F(0) - E_f - \frac{5}{18} n_0^{-1/3} F(0) \Delta n(r) \\ + \frac{25}{18} n_0^{-1/3} \int f(r-r') \Delta n(r') d^3r' + \Delta v(r) = 0, \end{aligned} \quad (2.9)$$

where  $F(0) = \int f(r) d^3r$ . The equation for the zeroth order is

$$F(0) = \frac{3}{5} n_0^{-2/3} E_f = \frac{3}{10} (3\pi^2)^{2/3}. \quad (2.10)$$

That is the condition we need to recover the TF theory when the density variation is slow. For the first order, transformed to  $k$  space, it becomes

$$-\frac{5}{18} n_0^{-1/3} F(0) \Delta N(k) + \frac{25}{18} n_0^{-1/3} F(k) \Delta N(k) + \Delta V(k) = 0, \quad (2.11)$$

and comparing to the linear-response result in Eq. (2.5), we have

$$-\frac{5}{18} n_0^{-1/3} F(0) + \frac{25}{18} n_0^{-1/3} F(k) - \frac{1}{G(k)} = 0. \quad (2.12)$$

Solving for  $F(k)$ ,

$$F(k) = \frac{18 n_0^{1/3}}{25} \frac{1}{G(k)} + \frac{1}{5} F(0), \quad (2.13)$$

and using the form for  $G(k)$ ,  $F(0)$ , and  $n_0$ , we find

$$F(k) = \frac{6}{25} (3\pi^2)^{2/3} \left[ \mathcal{W}^{-1} \left[ \frac{k}{k_F} \right] + \frac{1}{4} \right]. \quad (2.14)$$

Notice that, as  $z \rightarrow \infty$ ,

$$\mathcal{W}^{-1}(q) \rightarrow \frac{3}{4} q^2 - \frac{3}{5}, \quad (2.15)$$

and so  $f(r-r')$  contains a differential operator in real space. In order to get merely a function in real space, we can define another function  $\mathcal{W}_1(q)$  as

$$\mathcal{W}_1(q) = \frac{5}{8} \left[ \mathcal{W}^{-1}(q) - \frac{3}{4} q^2 + \frac{3}{5} \right], \quad (2.16)$$

then

$$F(k) = \frac{6}{25} (3\pi^2)^{2/3} \left[ \frac{8}{5} \mathcal{W}_1 \left[ \frac{k}{k_F} \right] + \frac{3}{4k_F^2} k^2 - \frac{7}{20} \right]. \quad (2.17)$$

Now back in real space, the  $k^2$  term is just  $\nabla^2$  and the constant term is a  $\delta$  function. Thus the expression in real space is

$$\begin{aligned} E_{\text{kin}} = \frac{48}{125} (3\pi^2)^{2/3} \int \int n^{5/6}(r) w_1(r-r') n^{5/6}(r') d^3r d^3r' \\ - \frac{21}{250} (3\pi^2)^{2/3} \int n^{5/3}(r) d^3r \\ - \frac{9}{50} n_0^{-2/3} \int n^{5/6}(r) \nabla^2 n^{5/6}(r) d^3r. \end{aligned} \quad (2.18)$$

where  $w_1(r-r')$  is the function  $\mathcal{W}_1(k)$  in real space. It is easy to show that up to quadratic order

$$-\frac{9}{50} n_0^{-2/3} \int n^{5/6}(r) \nabla^2 n^{5/6}(r) d^3r \Rightarrow -\frac{1}{2} \int n^{1/2}(r) \nabla^2 n^{1/2}(r) d^3r. \quad (2.19)$$

This is exactly the von Weizsäcker term. So, finally, the kinetic-energy functional can be written as

$$E_{\text{kin}}[n] = \frac{48}{125}(3\pi^2)^{2/3} \int \int n^{5/6}(r)w_1(r-r') \times n^{5/6}(r')d^3r d^3r' - \frac{21}{250}(3\pi^2)^{2/3} \int n^{5/3}(r)d^3r - \frac{1}{2} \int n^{1/2}(r)\nabla^2 n^{1/2}(r)d^3r. \quad (2.20)$$

(This will be referred to as the first-order formula in the following numerical comparisons.) The function  $w_1(r-r')$  in real space is shown in Fig. 1.

Now let us discuss briefly the properties of the above formula (2.20). It is very pleasing to see that the von Weizsäcker term comes out naturally. It is not a surprise for this term to come out correctly, however, because it is well known that the von Weizsäcker term can be derived from the linear-response theory of the high- $k$  region, and that is exactly what has been done above. Note the integral of  $w_1(r-r')$  is 1, so the first two terms sum to give the Thomas-Fermi term when the variation of density is slow. Thus the above formula can be thought of as a modification of Thomas-Fermi-von Weizsäcker (TFvW) theory. It is obvious in  $k$  space that the first term in Eq. (2.20) is always smaller than  $(48/125)(3\pi^2)^{2/3} \int n^{5/3}(r)d^3r$ , and the sum of the first two terms is always smaller than the Thomas-Fermi term. Thus the correction is in the right direction because the TFIW formula always over estimates of the kinetic energy. Derived as it is from linear-response theory, the above formula gives the exact response function for a small perturbation from the uniform electron gas, while TFvW theory or other gradient expansion formulas only gives the correct answer in part of the  $k$  region. It is easy to see that the above formula is not directly applicable to an isolated atom, because for that system the  $n_0$  in function  $w_1$  does not make any sense. We will discuss this point in the following section. However, for a typical solid system, the direct use of the above formula (1.20) with  $n_0$  set equal to the average electron density gives good results. This procedure is not

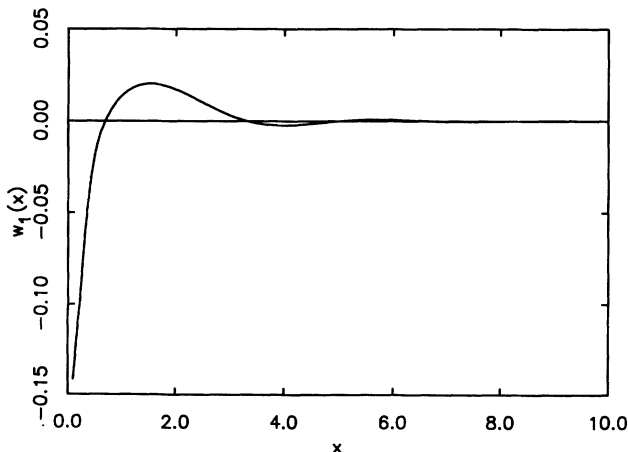


FIG. 1. Function  $w_1(k_F|r-r'|)$  in real space.

designed for use on isolated atoms, molecules, or surfaces, but rather for simulations of large condensed-matter systems.

Now some numerical results will be presented. An eight-atom silicon cube in the diamond structure is chosen as our example. Because the current formula can presently only work for local potentials, we use local pseudopotentials. Two local pseudopotentials will be used to test the valuable range of the above formula. The first pseudopotential is an often-used pseudopotential before the birth of the first-principles nonlocal pseudopotentials. It is obtained from Ref. 13, and has the form in  $k$  space

$$V_p(k) = Z \left[ \frac{a_1}{k^2} \right] [\cos(a_2 k) + a_3] e^{a_4 k^4}, \quad (2.21)$$

with

$$a_1 = -0.992, \quad a_2 = 0.791, \\ a_3 = -0.352, \quad a_4 = -0.018. \quad (2.22)$$

The second pseudopotential is a Starkloff-Joannopoulos pseudopotential with the form

$$V_p(r) = -\frac{Z}{r}(1 - e^{-\lambda r}) / (1 + e^{-\lambda(r-r_c)}), \quad (2.23)$$

with

$$\lambda = 31.192 \quad \text{and} \quad r_c = 1.060. \quad (2.24)$$

These two pseudopotentials are shown in Fig. 2. Actually, the second one is so sharp around  $r_c$ , for our numerical grid ( $16 \times 16 \times 16$ ), that it can be thought of as an Ashcroft<sup>14</sup> empty core pseudopotential. The self-consistent computations are carried out by using the plane-wave basis conjugate gradient method.<sup>15</sup> To solve the Kohn-Sham equations, eight  $k$  points are used, so there are 128 bands in the computations. Then the electron densities and total potentials are given by the results. Substituting these correct densities in the above kinetic-

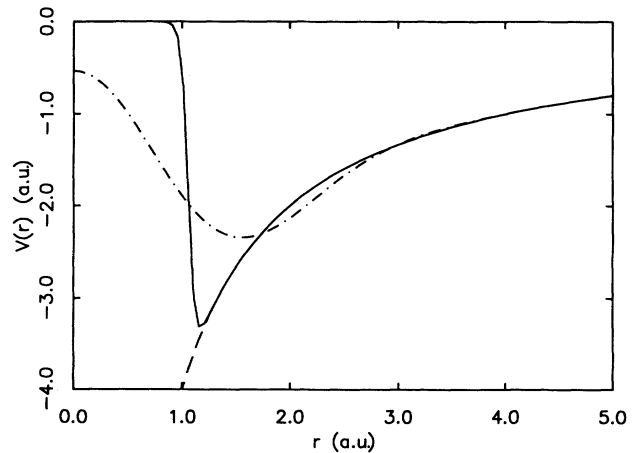


FIG. 2. Two pseudopotentials. The dash-dotted line is the first local pseudopotential. The solid line is the Starkloff-Joannopoulos pseudopotential. The dashed line is  $-4/r$ .

TABLE I. Total energies of different formulas for the smooth first pseudopotential system. Values are in hartree.

	Energy comparison for the first system		Energy drop
	Kohn-Sham density	Variational density	
Kohn-Sham result	$E_{\text{tot}} = 5.9926$ $E_{\text{kin}} = 11.5986$		
First-order formula	$E_{\text{tot}} = 6.3020$ $E_{\text{kin}} = 11.9080$	$E_{\text{tot}} = 6.1870$ $E_{\text{kin}} = 11.2264$	$\Delta E_{\text{tot}} = -0.1150$
Local $k_F$ formula	$E_{\text{tot}} = 6.1234$ $E_{\text{kin}} = 11.7294$	$E_{\text{tot}} = 6.0542$ $E_{\text{kin}} = 11.6275$	$\Delta E_{\text{tot}} = -0.0692$
Second-order formula	$E_{\text{tot}} = 6.0587$ $E_{\text{kin}} = 11.6647$	$E_{\text{tot}} = 6.0197$ $E_{\text{kin}} = 11.5075$	$\Delta E_{\text{tot}} = -0.0390$
TF $_{\frac{1}{5}}$ W	$E_{\text{tot}} = 6.0673$ $E_{\text{kin}} = 11.6732$	$E_{\text{tot}} = 5.7519$ $E_{\text{kin}} = 11.6439$	$\Delta E_{\text{tot}} = -0.3154$
TF $_{\frac{1}{9}}$ W	$E_{\text{tot}} = 5.7798$ $E_{\text{kin}} = 11.3858$	$E_{\text{tot}} = 5.3413$ $E_{\text{kin}} = 11.9742$	$\Delta E_{\text{tot}} = -0.4385$
TF1W	$E_{\text{tot}} = 8.6543$ $E_{\text{kin}} = 14.2602$	$E_{\text{tot}} = 7.2278$ $E_{\text{kin}} = 10.3373$	$\Delta E_{\text{tot}} = -1.4265$

energy formula, we get kinetic energies, and can compare them to the correct kinetic energies of the Kohn-Sham equations. The TF $\lambda$ W formula kinetic energies are also computed for  $\lambda = 1, \frac{1}{5}, \frac{1}{9}$ . The results are shown in column two of Tables I and II for the two pseudopotentials, respectively. Also in the table (and in other tables) are the results of the local  $k_F$  formula and the second-order formula, which will be discussed in the following sections. They are placed together to facilitate the comparison. We will come back to discuss those items later. For the first-order formula, as we can see, the kinetic energies computed by the exact densities are either worse than or slightly better than TF $_{\frac{1}{5}}$ W results, depending on the systems. The same is true when comparing to the TF $_{\frac{1}{9}}$ W results. But the first-order formula is much better than the full TF1W results. A more stringent test is in the quality of the densities that the formulas produce variationally. Using the above Kohn-Sham densities, we get the corresponding total potentials  $V_{\text{tot}}(r)$  for the systems, and they are shown in Figs. 3(a) and 3(b). The aver-

age variations  $\langle |[V(r) - V_0]| \rangle$  of these total potentials are 0.257 and 0.292 hartree, respectively. To isolate the effects of the kinetic-energy functional, we will use these total potentials to carry out non-self-consistent computations for the above formulas. These calculations have also been done self-consistently, and no significant difference was found. We used the same numerical method as for the Kohn-Sham equations to solve the variational densities of the kinetic-energy formulas. The variational densities computed by the first-order and TF $_{\frac{1}{5}}$ W formulas are shown in Figs. 4 and 5 for these two pseudopotential systems by the contour plots of the densities. Also in Figs. 4 and 5 are the Kohn-Sham exact densities and the results of the local  $k_F$  formula and the second-order formula in the following sections. The errors of the densities are computed by the error of density in real space

$$\frac{\sum |n_{\text{exact}}(r) - n_{\text{approx}}(r)|}{\sum n_{\text{exact}}(r)} \quad (2.25)$$

TABLE II. Total energies of different formulas for the sharp second pseudopotential system. Values are in hartree.

	Energy comparison for the second system		Energy drop
	Kohn-Sham density	Variational density	
Kohn-Sham result	$E_{\text{tot}} = 5.6852$ $E_{\text{kin}} = 11.8772$		
First-order formula	$E_{\text{tot}} = 5.8535$ $E_{\text{kin}} = 12.0454$	$E_{\text{tot}} = 5.5273$ $E_{\text{kin}} = 11.9517$	$\Delta E_{\text{tot}} = -0.3262$
Local $k_F$ formula	$E_{\text{tot}} = 5.6607$ $E_{\text{kin}} = 11.8526$	$E_{\text{tot}} = 5.3855$ $E_{\text{kin}} = 12.6003$	$\Delta E_{\text{tot}} = -0.2742$
Second-order formula	$E_{\text{tot}} = 5.6445$ $E_{\text{kin}} = 11.8365$	$E_{\text{tot}} = 5.4113$ $E_{\text{kin}} = 12.1007$	$\Delta E_{\text{tot}} = -0.2332$
TF $_{\frac{1}{5}}$ W	$E_{\text{tot}} = 5.4846$ $E_{\text{kin}} = 11.6765$	$E_{\text{tot}} = 4.2394$ $E_{\text{kin}} = 13.0372$	$\Delta E_{\text{tot}} = -1.2452$
TF $_{\frac{1}{9}}$ W	$E_{\text{tot}} = 5.1892$ $E_{\text{kin}} = 11.3812$	$E_{\text{tot}} = 3.4505$ $E_{\text{kin}} = 13.6531$	$\Delta E_{\text{tot}} = -1.7387$
TF1W	$E_{\text{tot}} = 8.1423$ $E_{\text{kin}} = 14.3342$	$E_{\text{tot}} = 6.7064$ $E_{\text{kin}} = 10.8595$	$\Delta E_{\text{tot}} = -1.4359$

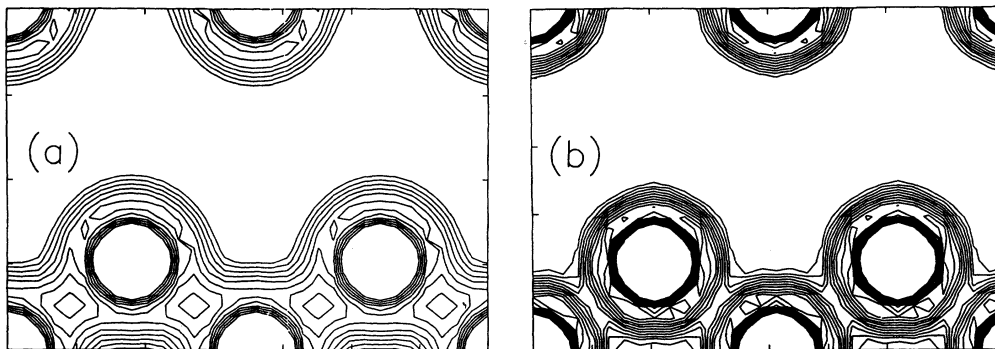


FIG. 3. The total potentials of the Kohn-Sham solutions. The cross section for the contour plot of [110] in the diamond cubic (the same for all the other contour plots). The contour plots only show negative potential contours for simplicity. The contour interval is 0.007 a.u. (a) First pseudopotential system, (b) Starkloff-Joannopoulos pseudopotential system. Note that there is a small well at each bonding area in (a).

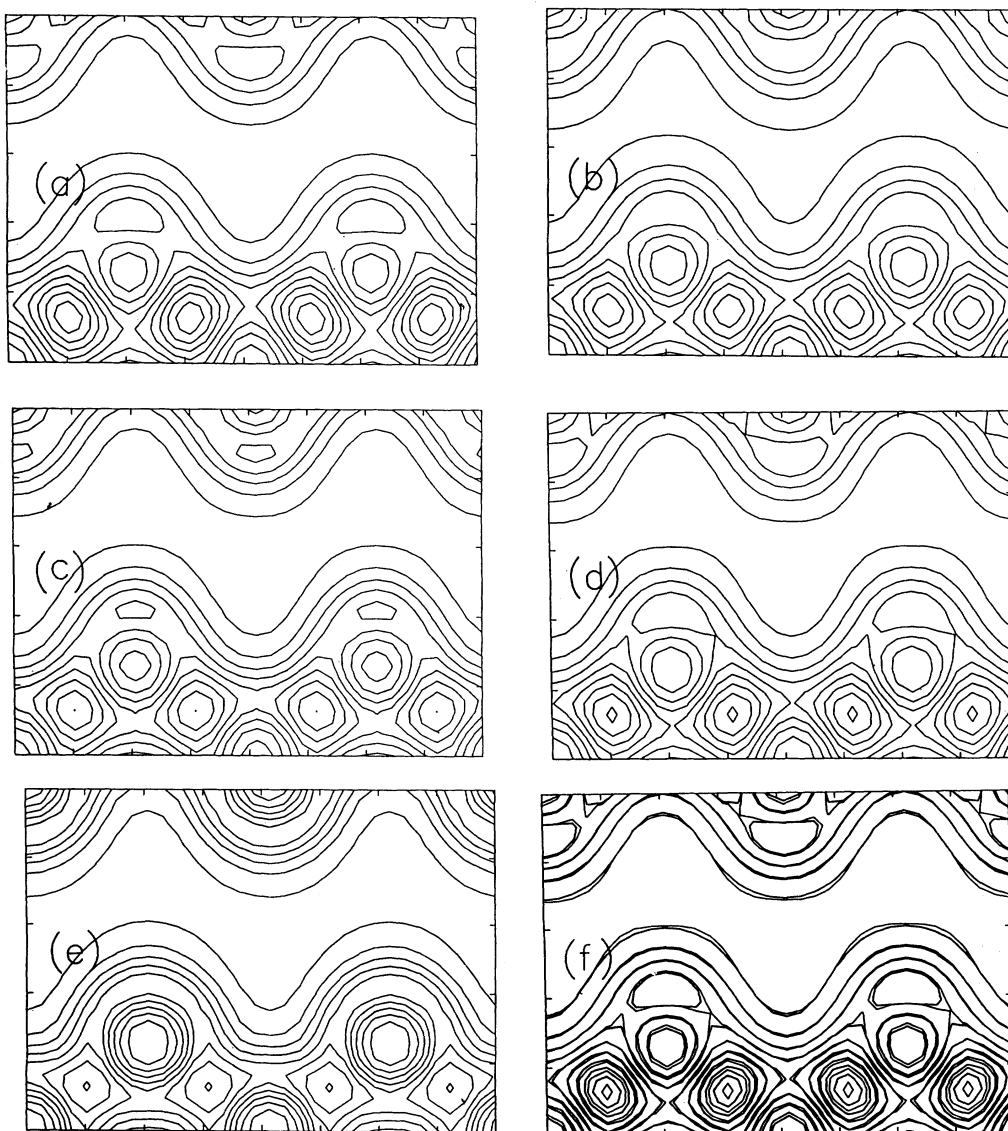


FIG. 4. Variational density contour plots of the first system for different formulas. They are all plotted in the same levels. The interval between two successive levels is 0.008 a.u. (a) Exact Kohn-Sham density, (b) first-order formula density, (c) local  $k_F$  formula density, (d) second-order formula density, (e)  $TF_5^1 W$  density, (f) comparison between the Kohn-Sham density and the second-order formula density.

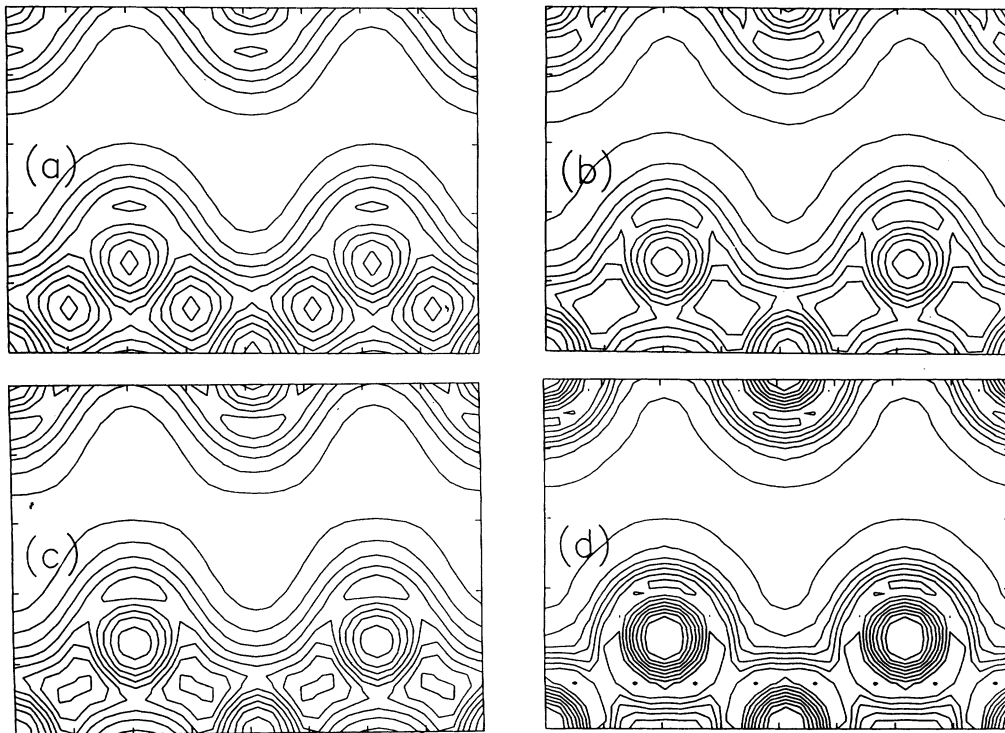


FIG. 5. Variational density contour plots of the second (Starkloff-Joannopoulos pseudopotential) system for different formulas. They are all plotted in the same levels. The interval between two successive levels is 0.008 a.u. (a) Exact Kohn-Sham density, (b) first-order formula density, (c) second-order formula density, (d)  $TF_{\frac{1}{5}}W$  density.

and the error of density in  $\mathbf{k}$  space

$$\frac{\sum |n_{\text{exact}}(k) - n_{\text{approx}}(k)|}{\sum |n_{\text{exact}}(k)|} \quad (2.26)$$

These errors are summarized in Table III for both pseudopotential systems (because of the limited space, only some of the results listed in the tables are shown in Figs.

TABLE III. Errors of variational densities according to Eqs. (2.25) and (2.26).

	Variational density errors	
	Second pseudopotential system	First pseudopotential system
First-order formula	$\Delta n(r) = 10.26\%$ $\Delta n(k) = 41.54\%$	$\Delta n(r) = 7.78\%$ $\Delta n(k) = 19.98\%$
Local $k_F$ formula	$\Delta n(r) = 11.00\%$ $\Delta n(k) = 49.45\%$	$\Delta n(r) = 6.43\%$ $\Delta n(k) = 21.95\%$
Second-order formula	$\Delta n(r) = 6.04\%$ $\Delta n(k) = 32.29\%$	$\Delta n(r) = 3.49\%$ $\Delta n(k) = 12.47\%$
$TF_{\frac{1}{5}}W$	$\Delta n(r) = 21.95\%$ $\Delta n(k) = 115.54\%$	$\Delta n(r) = 13.15\%$ $\Delta n(k) = 44.79\%$
$TF_{\frac{1}{9}}W$	$\Delta n(r) = 30.32\%$ $\Delta n(k) = 157.90\%$	$\Delta n(r) = 15.85\%$ $\Delta n(k) = 57.53\%$
TF1W	$\Delta n(r) = 25.54\%$ $\Delta n(k) = 51.55\%$	$\Delta n(r) = 25.89\%$ $\Delta n(k) = 45.85\%$

4 and 5, but they are all qualitatively similar). As shown in the table, for the first-order densities, the errors are reduced by a factor of 2 from the errors of  $TF_{\frac{1}{5}}W$  densities. Another interesting variable is the kinetic energy of the final variational density. These values are listed in the third column of Tables I and II. However, this variable mixes the initial correct density kinetic-energy results (column two of Tables I and II) with the variational process. As a result, a bad formula that has a large kinetic energy for the correct density might have an accurate final kinetic energy after the variational process and a large energy drop. So, a more interesting variable is the total energy drop from the initial exact density to the final variational density, as shown in column four of Tables I and II. This variable is a direct measure of the change in the variational process. It, like the density error values in Table III, represents the closeness of the initial exact density to the final variational density. If they are close, the energy drop is small, and vice versa. As shown in the table, the energy drop of the first-order formula is about a factor of 3 or 4 smaller than the energy drop of  $TF_{\frac{1}{5}}W$ . This is consistent with the density error comparison in Table III.

However, the most important feature of the density can only be seen in the density plots. Notice that there are bond charges in the present results, which are almost always absent in the  $TF\lambda W$  densities. The small bond charge for the first pseudopotential system of the  $TF\lambda W$  densities exists because there is a small well in the total potential [Fig. 3(a)]. We found out if we remove that

well, the TF $\lambda$ W variational densities will no longer have the bond charges, while the new formula results still have them. This can also be seen in Fig. 5 for the densities of the second pseudopotential system or in Fig. 12 for an amorphous system. In both cases, there is no well in the total potential, and there is no bond charge for the TF $\lambda$ W variational densities. So the bond-charge phenomena in our cases are purely the quantum-interference effects, and they loosely correspond to the shell structures in the atoms. These bond structures are, of course, very important to the chemistry. Although the bonds in the first-order-formula variational densities are still too small, they are probably the first such variational bonds computed by an approximate kinetic-energy functional in a real system, and this is regarded as the most important achievement of the current formula.

To get the right amplitude of the bond charge, we need to introduce the higher-order formulas. However, before doing that, we will introduce a way to adjust  $k_F$  in  $w_1$  according to the local density and to test how much improvement it can give. We will also apply our formula to isolated atoms after this modification.

### III. LOCAL DEPENDENCE OF $k_F$ AND APPLICATION TO ATOMS

In the previous section, we presented a new kinetic-energy functional of the charge density [Eq. (2.20)], which incorporated the Thomas-Fermi-von Weizsäcker formula with the linear-response theory. The function  $w_1(r-r')$  in that formula is defined in  $k$  space as

$$W_1(k) = \frac{5}{8} \left[ \left[ 0.5 + \frac{\left[ \left( \frac{k}{2k_F} \right)^2 - 1 \right]}{4 \left[ \frac{k}{2k_F} \right]} \ln \left| \frac{1 - \frac{k}{2k_F}}{1 + \frac{k}{2k_F}} \right| \right]^{-1} - 3 \left[ \frac{k}{2k_F} \right]^2 + \frac{3}{5} \right]. \quad (3.1)$$

However, here  $k_F$  is the Fermi momentum for the average density  $n_0$  of the system, i.e.,

$$k_F = (3\pi^2)^{1/3} n_0^{1/3}. \quad (3.2)$$

It may not be legitimate to use the average  $k_F$  when the system has large density variations, since the  $k_F$  in one place should be quite different from the  $k_F$  in another place. This is especially so when one tries to apply the above formula to an isolated system like an atom; in that case, the average density  $n_0$  does not make sense at all. In this section, a technique to solve this problem will be developed, which adjusts the  $k_F$  locally depending on the local density and is computationally affordable. This technique also has general applications to any similar problem.

First, the most straightforward method is to use some kind of average  $n(r)$  around point  $r$  and  $r'$  to get  $k_F$  (see

Ref. 11). But, to do this, we have to carry out the double integral directly. That is computationally expensive. Besides, there is no *a priori* reason to know what average should be used,  $[n(r)n(r')]^{1/2}$ ,  $\frac{1}{2}[n(r)+n(r')]$  or others. And, actually, none of them seems to do a good job. The technique we introduce below has no such problems. The local dependence of  $k_F$  looks natural, and it is faster to compute than a double integral. One drawback is that there is an approximation in the derivation. The accuracy depends on how many Gaussian functions are used to approximate the function  $W_1(k)$ . In practice, however, we found this is not a big problem. The results are not crucially dependent upon the approximation.

First let us consider  $w_1(r_0, r)$  as a wave or a Green's function that propagates from  $r_0$  to  $r$  in the medium  $n(r')$ , just like the light travels in a medium. Because, within the range  $r_0$  to  $r$ , the "index"  $n(r')$  of the medium has changed an appreciable amount, we do not know what  $n(r')$  should be used for  $k_F$ . However, let us assume that we can break down  $w_1(r_0, r)$  to  $N$  successive small propagators  $g(r_l, r_{l+1})$ :

$$w_1(r_0, r) = g(r_0, r_1) \prod_{l=1}^{N-1} \left[ \int d^3r_l g(r_l, r_{l+1}) \right], \quad (3.3)$$

where  $r_N = r$ . Then when  $N$  is large,  $g(r_l, r_{l+1})$  is local, and we can use  $n(r)$  around  $r_l, r_{l+1}$ , e.g.,  $[n(r_l)n(r_{l+1}))]^{1/2}$  to compute  $k_F$ . The  $g$  can be written as

$$g(r_l, r_{l+1}) = g(k_f |r_l - r_{l+1}|).$$

Now we must determine the most local propagator  $g(r_l, r_{l+1})$ . For a numerical computation, if we use a discrete mesh, the most local propagator is the propagator which only propagates to its nearest-neighbor points on the mesh. But one problem is that, for a homogeneous electron gas and a cubic mesh, after  $N$  successive convolutions of the nearest-neighbor propagator  $g$ , the result is not  $w_1(r_0, r)$ , but is a Gaussian function. To simulate

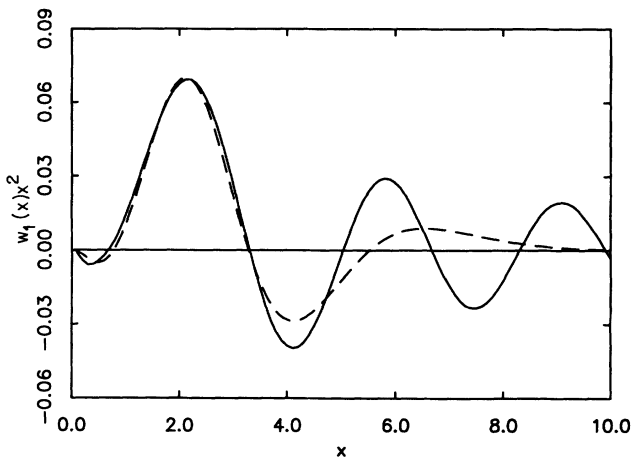


FIG. 6. An approximation of  $w_1(k_F|r-r'|)$  by several Gaussian functions in real space. What is shown in the graph is actually  $x^2 w_1(x)$ . The dashed line is the approximated result. The formula is  $w_1(x) = 0.179e^{-x^2/4.2} - 0.459e^{-x^2/9} + 0.3943e^{-x^2/9.4} - 0.1239e^{-x^2/1.9} - 0.04131e^{-x^2/0.3}$ .

$w_1(r_0, r)$ , we need a sum of several Gaussian functions as

$$w_1(k_F|r-r_0|) = \sum_{q=1}^m A_q \left[ \frac{k_F^3}{B_q^3 \pi^{3/2}} e^{-(k_F|r-r_0|)^2/B_q^2} \right]. \quad (3.4)$$

One such approximation is shown in Fig. 6. This approximation captures the most important features of  $w_1(r_0, r)$  within the region of several  $1/k_F$ . It is known from our experience that for  $|r-r_0|$  much larger than several  $1/k_F$  regions, usually the contributions from different places almost cancel out, so it is not very important. In terms of the propagators, we can rewrite  $w_1(r_0, r)$  as

$$w_1(r_0, r) = \sum_{q=1}^m A_q \left[ q(r_0, r_1) \prod_{l=1}^{N_q-1} \left[ \int d^3r_l g(r_l, r_{l+1}) \right] \right]. \quad (3.5)$$

Here  $r_{N_q} = r$  and  $N_q$  are the numbers of propagations corresponding to the Gaussian function  $B_q$ . Notice that the use of several Gaussian functions is not a serious drawback numerically. In order to compute the widest Gaussian function  $B_m$  by the nearest-neighbor propagation mentioned above, we need to consecutively compute the local propagator  $N_m$  times. During this computation, we must pass all other Gaussian functions which correspond to  $N_1, N_2, \dots, < N_m$ . A simple summation of those results as in Eq. (3.5) will give the  $w_1(r_0, r)$ .

To give a more detailed formula, we have, in the case of a homogeneous electron density  $n$ ,

$$g(i_l, i_{l+1}) = \delta_{i_{x_l}, i_{x_{l+1}}} \delta_{i_{y_l}, i_{y_{l+1}}} \delta_{i_{z_l}, i_{z_{l+1}}} c + (\delta_{i_{x_l} \pm 1, i_{x_{l+1}}} \delta_{i_{y_l}, i_{y_{l+1}}} \delta_{i_{z_l}, i_{z_{l+1}}} + \delta_{i_{x_l}, i_{x_{l+1}}} \delta_{i_{y_l} \pm 1, i_{y_{l+1}}} \delta_{i_{z_l}, i_{z_{l+1}}} + \delta_{i_{x_l}, i_{x_{l+1}}} \delta_{i_{y_l}, i_{y_{l+1}}} \delta_{i_{z_l} \pm 1, i_{z_{l+1}}}) b \quad (3.6)$$

and

$$\sum_{i_{l+1}} g(i_l, i_{l+1}) = 1, \quad (3.7)$$

so  $c = 1 - 6b$ .

The relation between  $b$  and  $B_q$  can be found by considering how the propagation forms the Gaussian function. It is easy to prove that

$$B_q = 2ak_F(N_q b)^{1/2}, \quad (3.8)$$

where  $a$  is the mesh lattice constant. Because  $k_F$  and  $b$  are the same for those different Gaussian functions, we immediately have

$$\frac{B_1^2}{N_1} = \frac{B_2^2}{N_2} = \dots = \frac{B_m^2}{N_m} \equiv \frac{B^2}{N}. \quad (3.9)$$

Using this equation, we can find corresponding  $N_q$  for the Gaussian functions. Now, for the inhomogeneous electron gas, we can change the above nearest-neighbor propagator  $g(i_l, i_{l+1})$  according to the local density by making  $k_F = (3\pi^2)^{1/3} n^{1/3}(r)$  in Eq. (3.8), with  $n(r)$  being the local density. So

$$b = \frac{B^2}{N} \frac{1}{(2a)^2} \frac{1}{(3\pi^2)^{2/3} n^{2/3}(r)} \equiv \frac{\alpha}{n^{2/3}(r)}. \quad (3.10)$$

More accurately,  $n^{2/3}$  should be the density between sites  $i_l$  and  $i_{l+1}$ , so the most proper choice is  $n(i_l)^{1/3} n(i_{l+1})^{1/3}$ . But there is a more general choice, which is  $n(i_l)^{(1/3)+\gamma} n(i_{l+1})^{(1/3)-\gamma}$ , and  $\gamma$  is a free parameter. This parameter represents a way not only to modify  $k_F$  according to the local density, but also to manipulate the formula according to the gradient of the local density. The nearest-neighbor propagator  $g(i_l, i_{l+1})$  with parameter  $\gamma$  will be denoted as  $g_\gamma(i_l, i_{l+1})$  and it is

$$g_\gamma(i_l, i_{l+1}) = \delta_{i_{x_l}, i_{x_{l+1}}} \delta_{i_{y_l}, i_{y_{l+1}}} \delta_{i_{z_l}, i_{z_{l+1}}} c + \delta_{i_{x_l} \pm 1, i_{x_{l+1}}} \delta_{i_{y_l}, i_{y_{l+1}}} \delta_{i_{z_l}, i_{z_{l+1}}} b_1 + \delta_{i_{x_l} - 1, i_{x_{l+1}}} \delta_{i_{y_l}, i_{y_{l+1}}} \delta_{i_{z_l}, i_{z_{l+1}}} b_2 + \delta_{i_{x_l}, i_{x_{l+1}}} \delta_{i_{y_l} + 1, i_{y_{l+1}}} \delta_{i_{z_l}, i_{z_{l+1}}} b_3 + \delta_{i_{x_l}, i_{x_{l+1}}} \delta_{i_{y_l} - 1, i_{y_{l+1}}} \delta_{i_{z_l}, i_{z_{l+1}}} b_4 + \delta_{i_{x_l}, i_{x_{l+1}}} \delta_{i_{y_l}, i_{y_{l+1}}} \delta_{i_{z_l} + 1, i_{z_{l+1}}} b_5 + \delta_{i_{x_l}, i_{x_{l+1}}} \delta_{i_{y_l}, i_{y_{l+1}}} \delta_{i_{z_l} - 1, i_{z_{l+1}}} b_6, \quad (3.11)$$

with

$$b_{1,\dots,6} = \frac{\alpha}{n(i_l)^{(1/3)+\gamma} n(i_{l+1})^{(1/3)-\gamma}}, \quad (3.12)$$

where

$$\alpha = \frac{B^2}{N} \frac{1}{(2a)^2 (3\pi^2)^{2/3}}$$

and

$$c = 1 - b_1 - b_2 - b_3 - b_4 - b_5 - b_6. \quad (3.13)$$

However, notice that

$$n(i_l)^{2\gamma} g_\gamma(i_l, i_{l+1}) = n(i_{l+1})^{2\gamma} g_\gamma(i_{l+1}, i_l). \quad (3.14)$$

As a result, the  $w_1(r_0, r)$  defined in (3.4) is not symmetrized. To get a symmetry  $w_1(r_0, r)$ , we can redefine it as

$$w_1(r_0, r) = n(r_0)^\gamma G_\gamma(r_0, r) n(r)^{-\gamma}, \quad (3.15)$$

and  $G_\gamma(i_0, i)$  is defined as

$$G_\gamma(i_0, i) = \sum_{q=1}^m A_q \left[ g_\gamma(i_0, i_1) \prod_{l=1}^{N_q-1} \left[ \sum_{i_l} g_\gamma(i_l, i_{l+1}) \right] \right], \quad (3.16)$$

with  $i_{N_q} = i$ .

Finally, the process to compute

$$F_2(r_0) = \int w_1(r_0, r) F_1(r) d^3r \quad (3.17)$$

is clear. First, we can rewrite it as

$$f'(r_0) = \int G(r_0, r) f(r) d^3r. \quad (3.18)$$

Here  $f(r) = n(r)^{-\gamma} F_1(r)$  and  $f'(r_0) = n(r_0)^{-\gamma} F_2(r_0)$ . To compute (3.18), we need to compute

$$f_{l+1}(i_{l+1}) = \sum_{i_l} f_l(i_l) g_\gamma(i_l, i_{l+1}) \quad (3.19)$$

successively for  $N_m$  times [with  $f(i)$  as  $f_0(i)$ ], and sum up  $f_{N_q}(i)$  according to (3.16). So the result is

$$f'(i) = \sum_{q=1}^m A_q f_{N_q}(i). \quad (3.20)$$

Now, with respect to numerical efficiency, because  $b$  cannot be too large ( $< 0.15$ ) (in order to keep the resulting  $N$  successive convolution of  $g$  being close to a Gaussian function), the number of times ( $N_m$ ) to execute the nearest-neighbor propagator depends on how large  $B_m$  is and how fine the mesh lattice  $a$  is comparing to the characteristic length of the density  $n$ . In our case, for a reasonable accuracy,  $N_m$  is about 90. In the region where  $n(i)$  is extremely small,  $b$  according to above formula could be larger than 0.15. In that case, make  $b$  equal or less than 0.15, but keep Eqs. (3.13) and (3.14) satisfied. That will give a satisfactory result. For a  $N_m$  like 90, the computation to carry out Eq. (3.18) is about  $7 \times 90 \times N_{\text{mesh}}^3$ . Comparing to the using of the fast

Fourier transform to carry out a convolution, which is about  $2 \ln N_{\text{mesh}}^3 \times N_{\text{mesh}}^3$ , this method is about ten times slower for the system we studied, but is still affordable. And this method is much faster than the direct double-integral computation.

Now, substituting the above expression of  $w_1(r_0, r)$  to the original kinetic-energy functional (2.20), we have

$$E_{\text{kin}}[n] = a_1 \int \int n(r)^{(5/6)+\gamma} G_\gamma(r, r') n(r')^{(5/6)-\gamma} d^3r d^3r' - b_1 \int n^{5/3}(r) d^3r - \frac{1}{2} \int n^{1/2}(r) \nabla^2 n^{1/2}(r) d^3r. \quad (3.21)$$

(This will be referred to as the local  $k_F$  formula with  $\gamma$  in the following numerical comparisons.)  $G_\gamma(r, r')$  is defined as above, and has the following properties:

$$[n(r)]^\gamma G_\gamma(r, r') [n(r')]^{-\gamma} = [n(r')]^\gamma G_\gamma(r', r) [n(r)]^{-\gamma}, \quad (3.22)$$

and

$$\int G_\gamma(r, r') d^3r' = 1. \quad (3.23)$$

However, because of  $\gamma$ , if we carry out the lowest-order expansion around the uniform density  $n_0$  using Eqs. (3.22) and (3.23) and the fact that  $G_\gamma(r, r')$  equals  $w_1(r-r')$  when  $n(r) = n_0$ , then we will find out that in order to get the correct lowest-order expansion,  $a_1$  and  $b_1$  should not be the coefficients in Eq. (2.20); rather, they should be

$$a_1 = \frac{48}{125} (3\pi^2)^{2/3} (1 - \frac{6}{5}\gamma)^{-2}, \quad (3.24)$$

$$b_1 = a_1 - \frac{3}{10} (3\pi^2)^{2/3}.$$

Notice that, when  $\gamma=0$ ,  $a_1$  and  $b_1$  go back to the coefficients in Eq. (2.20). The fact that  $\gamma$  can change the values of  $a_1$  and  $b_1$  is very interesting. For example, when  $\gamma = (5 - 4\sqrt{2}) \frac{1}{6} \approx -0.10947$ ,  $b_1$  is zero. This is interesting because the existence of the  $b_1$  term is somehow not being appreciated. At any rate,  $\gamma$  provides one free parameter to adjust, and hopefully it could be useful. The numerical aspect of computing Eq. (3.21) has been discussed above. However, to compute the density  $n(r)$  variationally from the kinetic-energy functional (3.21), we need to compute the density derivative of  $G_\gamma(r, r')$ . Using Eq. (3.16) and the expression of  $g_\gamma(r_l, r_{l+1})$  in Eqs. (3.11), (3.12), and (3.13), we can write down the derivative of  $G_\gamma(r, r')$ . To simplify the notation, let us first define

$$\bar{G}_\gamma^N(i_0, i) = g_\gamma(i_0, i_1) \prod_{l=1}^{N-1} \left[ \sum_{i_l} g_\gamma(i_l, i_{l+1}) \right], \quad (3.25)$$

$$F_\gamma^N(i) = \sum_{i_0} [n(i_0)]^{(5/6)+\gamma} \bar{G}_\gamma^N(i_0, i). \quad (3.26)$$

In the notation of mesh index  $i$ , the first term in Eq. (3.21) can be rewritten as

$$\sum_{i_1} \sum_{i_2} [n(i_1)]^{(5/6)+\gamma} G_\gamma(i_1, i_2) [n(i_2)]^{(5/6)-\gamma}. \quad (3.27)$$

Then the derivative of  $G_\gamma(i_1, i_2)$  in this term is

$$\begin{aligned}
\sum_{i_1} \sum_{i_2} [n(i_1)]^{(5/6)+\gamma} \frac{\delta}{\delta n(i)} G_\gamma(i_1, i_2) [n(i_2)]^{(5/6)-\gamma} &= \sum_{q=1}^m A_q \left[ \sum_{i_1} \sum_{i_2} [n(i_1)]^{(5/6)+\gamma} \frac{\delta}{\delta n(i)} \bar{G}_\gamma^N(i_1, i_2) [n(i_2)]^{(5/6)-\gamma} \right] \\
&= \sum_{q=1}^m A_q \left[ \sum_{j=1}^{N_q} F_\gamma^j(i) F_\gamma^{N_q-j}(i) \left\{ -\frac{2}{3} [n(i)]^{-1-2-\gamma} \right\} \right. \\
&\quad \left. + \sum_{i'} \left[ \sum_{j=1}^{N_q} F_\gamma^{j-1}(i') F_\gamma^{N_q-j}(i') [n(i')]^{-2\gamma} \right] \right] \\
&\quad \times \left\{ \left[ \left( \frac{1}{3} + \gamma \right) \delta_{i',i} + \left( \frac{1}{3} - \gamma \right) g_\gamma(i', i) \right] [n(i)]^{-1} \right\}. \quad (3.28)
\end{aligned}$$

It needs the same order of computation as Eq. (3.22) but increased by a factor of 2 or 3. The variational equation for the square root of the density  $u(r) \equiv n^{1/2}(r)$  can be written down explicitly as

$$\begin{aligned}
\left[ \frac{5}{3} a_1 [n(r)]^{-(1/6)-\gamma} \int [n(r_1)]^{(5/6)+\gamma} G_\gamma(r_1, r) d^3 r_1 - \frac{5}{3} b_1 n^{2/3}(r) \right. \\
\left. + a_1 \int \int [n(r_1)]^{(5/6)+\gamma} \frac{\delta}{\delta n(r)} G_\gamma(r_1, r_2) [n(r_2)]^{(5/6)-\gamma} d^3 r_1 d^3 r_2 \right] u(r) - \frac{1}{2} \nabla^2 u(r) + v(r) u(r) = E_f u(r). \quad (3.29)
\end{aligned}$$

This is the equation to be used to compute  $u(r)$ . The equation having this form with the term in the large parentheses as an effective potential  $v_{\text{eff}}$  has been discussed before.<sup>16</sup> It is found that, when applying to an isolated system, the correct  $v_{\text{eff}}$  must be zero when  $r \rightarrow \infty$ , and it must be positive everywhere. The properties of  $v_{\text{eff}}$  in our formula will be discussed when we apply this formula to isolated atoms.

First, let us apply this formula to the silicon (diamond structure) system we computed in the last section. The results are not very sensitive to  $\gamma$  as long as we avoid  $\gamma$ 's that cause large values of  $a_1$  and  $b_1$  (which cause large number cancellations). In the following, we only give  $\gamma=0$  results. The kinetic energies for the correct densities are given in column two of Tables I and II. They are better than the direct first-order results. But it is difficult to know how reliable these numbers are, because the approximation for  $w_1(r-r')$  with some Gaussian functions in Fig. 6 has the same order of error as the kinetic functional itself, so the results could be accidental. Thus we should concentrate on the variational density results. Note the total energy drop in the fourth column of Tables I and II for this local  $k_F$  method is smaller than the direct first-order results. That is an improvement. A density contour is given in Fig. 4(c) for the first system, and the density errors are shown in Table III. The improvements on density errors depend on the systems. For the first system, the results get better, but for the second system, the density errors get even slightly larger. Examining the results more closely, however, we can find out that in both cases, the densities in the tail region are improved. That is encouraging, because that means this new formula can indeed adjust the  $k_F$  according to the local density, and so it can work for both the high- and low- $n(r)$  regions. On the other hand, the bond density is still lower than required. This probably means that this

problem is not due to the constant  $k_F$ , but is due to some other factors, perhaps the higher-order effects. In conclusion, this local  $k_F$  formula does show some improvements upon the original first-order formula for the solid systems. But the improvements are limited.

The real advantage of the  $k_F$  local dependent formula over the  $n_0$  one is that the new formula can be applied to isolated atoms. Because of the spherical symmetry of the atomic density, we can reduce the problem to one dimension. While the conception of the above propagation process is unchanged, the formulas can be simplified. Let  $r$  be the radial coordinate, and let  $i$  be the index of the one-dimensional mesh on  $r$ . How should we implement Eq. (3.21) in this one dimension  $r$ ? Starting with Eq. (3.21), the problem is to compute the integral  $\int [n(r)]^{(5/6)+\gamma} G_\gamma(r, r') d^3 r$  in the radial coordinate. First, this integral can be divided into several integrals of  $\bar{G}_\gamma^N(r, r')$ , as defined in (3.25). However, when the density is uniform,  $\bar{G}_\gamma^N(r, r')$  is just a Gaussian function, so the effect of the integral  $\int d(r) \bar{G}_\gamma^N(r, r') d^3 r$  is equivalent to solving the diffusion equation:

$$\frac{d}{dt} d(r, t) = -\beta \nabla^2 d(r, t), \quad (3.30)$$

with  $d(r, 0) \equiv d(r)$  and  $d(r, T)$  the result of the integral. The relation of  $\beta$  and  $T$  with the width of the Gaussian function can be easily found out. The above diffusion equation is well defined in the radial coordinate  $r$ ; actually, the solution can also be computed by consecutive applications of a nearest-neighbor propagator in the dimension  $r$ . When  $n(r)$  is not uniform, the effect of local  $n(r)$  and  $\gamma$  can be represented in the same way as in three dimensions. So, the integral  $\int d(r) \bar{G}_\gamma^N(r, r') d^3 r$  can be carried out in the radial coordinate. The detailed forms are given as

$$\int d(r) \bar{G}_\gamma^N(r, r') d^3r = \frac{1}{r_i'} \left[ \sum_i d(i) r_i \bar{H}_\gamma^N(i, i') \right]. \quad (3.31)$$

The  $\bar{H}_\gamma^N(i, i')$  is defined by

$$\bar{H}_\gamma^N(i_0, i) = h_\gamma(i_0, i_1) \prod_{l=1}^{N-1} \left[ \sum_{i_l} h_\gamma(i_l, i_{l+1}) \right], \quad (3.32)$$

where  $i_N = i$  and  $h_\gamma(i_l, i_{l+1})$  is the nearest-neighbor propagator:

$$h_\gamma(i, i') = \delta_{i-1, i'} b_{-1} + \delta_{i, i'} b_0 + \delta_{i+1, i'} b_{+1}, \quad (3.33)$$

with

$$b_{-1} = \frac{\alpha_1}{(r_i - r_{i-1})(r_i - r_{i-2}) n(i)^{(1/3) + \gamma} n(i-1)^{(1/3) - \gamma}},$$

$$b_{+1} = \frac{\alpha_1}{(i_{i+1} - r_i)(r_{i+2} - r_i) n(i)^{(1/3) + \gamma} n(i+1)^{(1/3) - \gamma}}, \quad (3.34)$$

$$b_0 = 1 - \frac{b_{+1}(r_{i+2} - r_i)r_{i+1} + b_{-1}(r_i - r_{i-2})r_{i-1}}{(r_{i+1} - r_{i-1})r_i},$$

where

$$\alpha_1 = \frac{B^2}{N} \frac{1}{2(3\pi^2)^{2/3}}$$

and  $B^2/N$  is the value in Eq. (3.9). Finally,

$$\begin{aligned} \int d(r) G_\gamma(r, r') d^3r &= \sum_{q=1}^m A_q \left[ \int d(r) \bar{G}_\gamma^{Nq}(r, r') d^3r \right] \\ &= \sum_{q=1}^m A_q \frac{1}{r_i'} \left[ \sum_i d(i) r_i \bar{H}_\gamma^{Nq}(i, i') \right]. \end{aligned} \quad (3.35)$$

The derivative of  $G_\gamma(r, r')$  by  $n(r)$  can be written in the same way as Eq. (3.28). Now, after knowing how to compute the integral in Eq. (3.29), the remaining terms are simple, because they all can be written down in the radial coordinate  $r$  very easily. To simplify the matter, hydrogenic atoms are chosen to be the examples; i.e., the total potential is  $-1/r$ , and the systems are computed non-self-consistently. Then the analytical solutions for various occupations are known. Using the correct densities, we can compute the kinetic energies by the above formulas and the TF $\lambda$ W formulas. The results are shown in Tables IV–VI. This time, we give both the  $\gamma=0$  and  $-0.10947$  results. The kinetic-energy errors of the new formula are about of the same order as the TF $\frac{1}{5}$ W results, and are better than the TF $\frac{1}{5}$ W and TF1W results (which we did not show, but the situation is very much like the solid systems in Tables I and II).

The variational densities are also computed based on Eq. (3.29). It is solved on a grid by a numerical integrator based on the term  $-\frac{1}{2}\nabla^2 u(r)$  in Eq. (3.29) and treating all other terms as an effective potential, and iterating this effective potential until it converged. The energy

drops in column four of Tables IV–VI are smaller for the current formula than the TF $\frac{1}{5}$ W results. This indicates the densities are better in this sense. The density profiles for  $1s^2$ ,  $1s^2 2s^2 2p^6$ , and  $1s^2 2s^2 2p^6 3s^2 3p^6 3d^{10}$  are shown, respectively, in Figs. 7, 8, and 9 for different formulas. Again, to limit the space, only some of the results are shown. Note that the new formula densities have humps

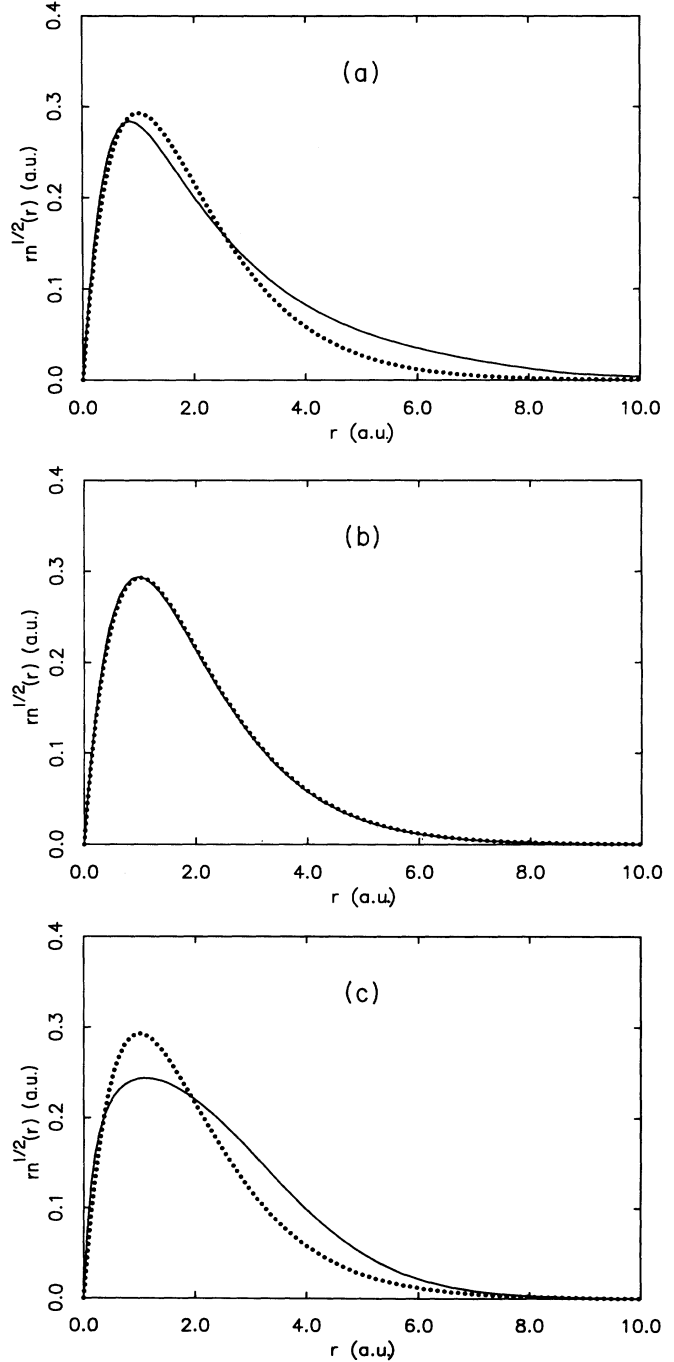


FIG. 7. Electron density profiles  $rn^{1/2}(r)$  of atom  $1s^2$  for different formulas. See Table IV for the corresponding energies. The dotted lines are the exact densities. (a) Local  $k_F$ ,  $\gamma=0$  density, (b) local  $k_F$ ,  $\gamma=0$  variational density without the  $(\partial/\partial n)G_\gamma$  term in Eq. (3.30), (c) TF $\frac{1}{5}$ W density.

TABLE IV. Energies of atom  $1s^2$  for different formulas.

	Energy comparison for atom $1s^2$		Energy drop and $E_F$
	Exact density	Variational density	
Exact	$E_{\text{tot}} = -1$ $E_{\text{kin}} = 1$		$E_F = -0.5000$
Local $k_F$ $\gamma = -0.10947$	$E_{\text{tot}} = -0.9578$ $E_{\text{kin}} = 1.0422$	$E_{\text{tot}} = -0.9729$ $E_{\text{kin}} = 0.9954$	$\Delta E_{\text{tot}} = -0.0151$ $E_F = -0.2982$
Local $k_F$ $\gamma = 0$	$E_{\text{tot}} = -0.9781$ $E_{\text{kin}} = 1.0219$	$E_{\text{tot}} = -0.9985$ $E_{\text{kin}} = 1.0338$	$\Delta E_{\text{tot}} = -0.0204$ $E_F = -0.2090$
Local $k_F$ , $\gamma = 0$ without $[(\partial/\partial n)G_\gamma(r, r')]$	$E_{\text{tot}} = -0.9781$ $E_{\text{kin}} = 1.0219$	$E_{\text{tot}} = -0.9806$ $E_{\text{kin}} = 1.0661$	$\Delta E_{\text{tot}} = -0.0025$ $E_F = -0.4933$
Modified formula $\gamma = -0.10947$	$E_{\text{tot}} = -1.0384$ $E_{\text{kin}} = 0.9616$	$E_{\text{tot}} = -1.1576$ $E_{\text{kin}} = 1.1200$	$\Delta E_{\text{tot}} = -0.1192$ $E_F = -0.1818$
Modified formula $\gamma = 0$	$E_{\text{tot}} = -0.9659$ $E_{\text{kin}} = 1.0341$	$E_{\text{tot}} = -1.0621$ $E_{\text{kin}} = 1.0143$	$\Delta E_{\text{tot}} = -0.0962$ $E_F = -0.1899$
TF $_{\frac{1}{5}}$ W	$E_{\text{tot}} = -0.8829$ $E_{\text{kin}} = 1.1171$	$E_{\text{tot}} = -0.9559$ $E_{\text{kin}} = 0.9559$	$\Delta E_{\text{tot}} = -0.0730$ $E_F = -0.2322$

TABLE V. Energies of atom  $1s^2 2s^2 2p^6$  for different formulas.

	Energy comparison for atom $1s^2 2s^2 2p^6$		Energy drop and $E_F$
	Exact density	Variational density	
Exact	$E_{\text{tot}} = -2$ $E_{\text{kin}} = 2$		$E_F = -0.1250$
Local $k_F$ $\gamma = -0.10947$	$E_{\text{tot}} = -1.9430$ $E_{\text{kin}} = 2.0570$	$E_{\text{tot}} = -1.9516$ $E_{\text{kin}} = 1.9895$	$\Delta E_{\text{tot}} = -0.0086$ $E_F = -0.0905$
Local $k_F$ $\gamma = 0$	$E_{\text{tot}} = -2.0008$ $E_{\text{kin}} = 1.9992$	$E_{\text{tot}} = -2.0073$ $E_{\text{kin}} = 2.0272$	$\Delta E_{\text{tot}} = -0.0065$ $E_F = -0.1002$
Modified formula $\gamma = -0.10947$	$E_{\text{tot}} = -1.9868$ $E_{\text{kin}} = 2.0132$	$E_{\text{tot}} = -2.0863$ $E_{\text{kin}} = 2.0425$	$\Delta E_{\text{tot}} = -0.0995$ $E_F = -0.0829$
Modified formula $\gamma = 0$	$E_{\text{tot}} = -1.9690$ $E_{\text{kin}} = 2.0310$	$E_{\text{tot}} = -2.0500$ $E_{\text{kin}} = 2.0396$	$\Delta E_{\text{tot}} = -0.0810$ $E_F = -0.0851$
TF $_{\frac{1}{5}}$ W	$E_{\text{tot}} = -1.8990$ $E_{\text{kin}} = 2.1010$	$E_{\text{tot}} = -1.9604$ $E_{\text{kin}} = 1.9519$	$\Delta E_{\text{tot}} = -0.0614$ $E_F = -0.0815$

TABLE VI. Energies of atom  $1s^2 2s^2 2p^6 3s^2 3p^6 3d^{10}$  for different formulas.

	Energy comparison for atom $1s^2 2s^2 2p^6 3s^2 3p^6 3d^{10}$		Energy drop and $E_F$
	Exact density	Variational density	
Exact	$E_{\text{tot}} = -3$ $E_{\text{kin}} = 3$		$E_F = -0.0555$
Local $k_F$ $\gamma = -0.10947$	$E_{\text{tot}} = -3.1037$ $E_{\text{kin}} = 2.8963$	$E_{\text{tot}} = -3.1215$ $E_{\text{kin}} = 3.1702$	$\Delta E_{\text{tot}} = -0.0178$ $E_F = -0.0484$
Local $k_F$ $\gamma = 0$	$E_{\text{tot}} = -3.2060$ $E_{\text{kin}} = 2.7940$	$E_{\text{tot}} = -3.2444$ $E_{\text{kin}} = 3.2831$	$\Delta E_{\text{tot}} = -0.0384$ $E_F = -0.0496$
Modified formula $\gamma = -0.10947$	$E_{\text{tot}} = -3.0191$ $E_{\text{kin}} = 2.9809$	$E_{\text{tot}} = -3.1112$ $E_{\text{kin}} = 3.0532$	$\Delta E_{\text{tot}} = -0.0921$ $E_F = -0.0427$
Modified formula $\gamma = 0$	$E_{\text{tot}} = -3.0125$ $E_{\text{kin}} = 2.9875$	$E_{\text{tot}} = -3.0868$ $E_{\text{kin}} = 3.0804$	$\Delta E_{\text{tot}} = -0.0743$ $E_F = -0.0428$
TF $_{\frac{1}{5}}$ W	$E_{\text{tot}} = -2.9054$ $E_{\text{kin}} = 3.0946$	$E_{\text{tot}} = -2.9599$ $E_{\text{kin}} = 2.9467$	$\Delta E_{\text{tot}} = -0.0545$ $E_F = -0.0412$

corresponding to the  $n=1$  and 2 levels. Especially for  $\gamma=0$ ,  $1s^2 2s^2 2p^6$  [Fig. 8(a)], the density is very close to the exact one (but for  $\gamma=-0.10947$ , the result is slightly worse than this one). Although it is very small, like in the solid system, it is the first time one can use a kinetic-energy functional to get such shell structures in the variational densities for such three-dimensional systems. Still, it fails to give the shell structure between the  $n=2$  and 3

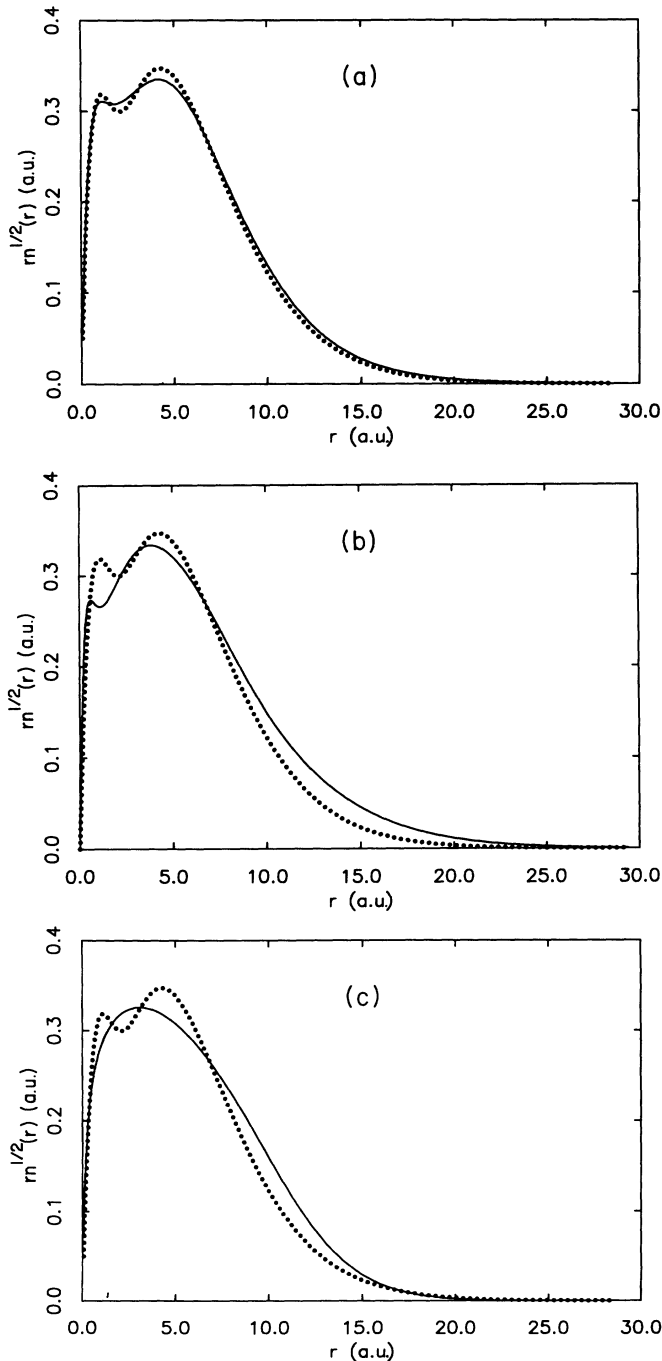


FIG. 8. Electron density profiles  $rn^{1/2}(r)$  of atom  $1s^2 2s^2 2p^6$  for different formulas. See Table V for the corresponding energies. The dotted lines are the exact densities. (a) Local  $k_F$ ,  $\gamma=0$  density, (b) modified formula,  $\gamma=0$  density, (c)  $TF_{\frac{1}{2}}W$  density.

levels in  $1s^2 2s^2 2p^6 3s^2 3p^6 3d^{10}$ , but it can give a shoulder corresponding to the  $n=3$  level, as we will discuss below. Besides, the new formulas get better Fermi energies than the  $TF\lambda W$  do. That means the densities in the tail region are better for the new formulas than the  $TF\lambda W$  results.

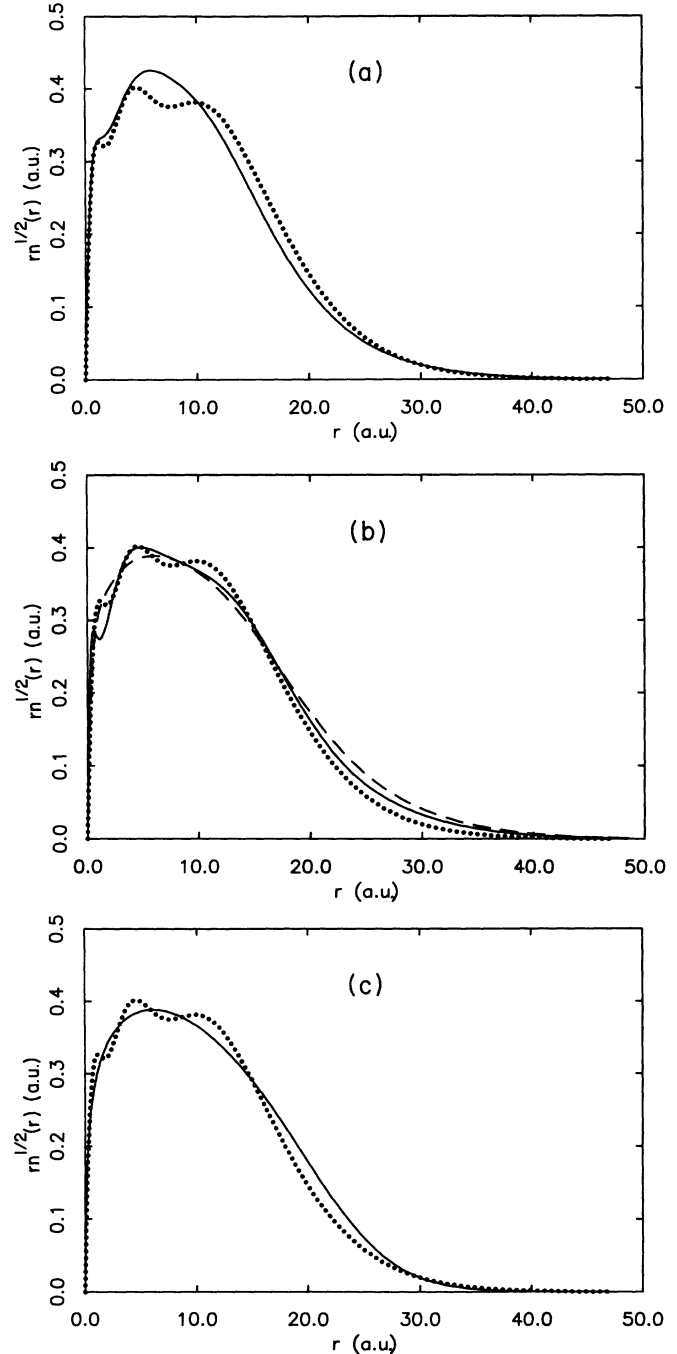


FIG. 9. Electron density profiles  $rn^{1/2}(r)$  of atom  $1s^2 2s^2 2p^6 3s^2 3p^6 3d^{10}$  for different formulas. See Table VI for the corresponding energies. The dotted lines are the exact densities. (a) Local  $k_F$ ,  $\gamma=-0.10947$  density, (b) modified formula,  $\gamma=-0.10947$  density (solid line). The dashed line is the variational density after the  $W'_1$  integral term is replaced by the Thomas-Fermi term. Note the shoulder of the solid line. (c)  $TF_{\frac{1}{2}}W$  density.

Of course, the Fermi energy itself is a very important chemical value. Another improvement over the TF $\lambda$ W results is for the  $r=0$  densities, which are the slopes near zero in the  $rn(r)$  profile curves. Note that the new formulas get almost the exact densities for  $r=0$ .

Shown in Fig. 10 is the effective potential  $v_{\text{eff}}$  defined in the large parentheses in Eq. (3.29) for atom  $1s^22s^22p^6$ . As can be seen,  $v_{\text{eff}}$  does not go to zero when  $r$  goes to infinity. This is caused by the  $(\delta/\delta n)G$  term in Eq. (3.29). This happens in the region when we have to fix  $b_{+1}$  numerically (see the discussion below). As a result of this fixing, Eq. (3.28) no longer holds for this region. But that equation was used to compute the  $v_{\text{eff}}$  in Fig. 10. So it is not absolutely clear whether it is the numerical error or the formula itself which causes the blowup of  $v_{\text{eff}}$ . But, in any case, this indicates that the formula has some difficulties in the very small density region. Fortunately, this blowup of  $v_{\text{eff}}$  is sufficiently out in  $r$  that it does not have a big effect on the density profiles. Also note that, for some  $\gamma$ 's, there might be a small negative region of  $v_{\text{eff}}$  near the nuclei.

Also included in Tables IV–VII and Figs. 8 and 9 are the results of a modified formula that is used to try to improve the smallness of the shell structure in the above results. The same kind of modification for a solid system will be encountered in the next section. Notice that in our formula (3.29), we have the full von Weizsäcker term over all space. However, it is well known that, in the atoms, in the middle region (not the tail, not the nuclei), when  $|\nabla n|/n^{4/3} < 1$ , the  $\frac{1}{9}$  von Weizsäcker term is appropriate. So the task is how to incorporate the second-order gradient expansion term into our formula in such an apparent way. To do that, we can add a term:

$$T_{\text{add}} = -\left(\frac{8}{9}\right)^{\frac{1}{2}} \sum_k k^2 f\left[\frac{k}{k_F}\right] \times \left[ n^{1/2}(k)n^{1/2}(k) - \left(\frac{3}{5}\right)^2 \frac{1}{n_0^{2/3}} n^{5/6}(k)n^{5/6}(k) \right]. \quad (3.36)$$

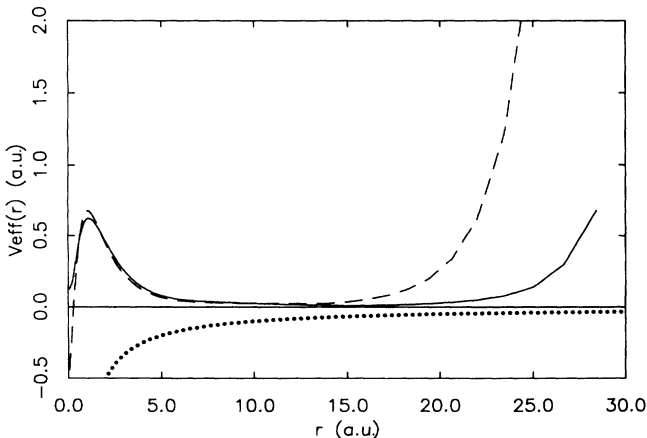


FIG. 10. Effective potential  $v_{\text{eff}}$  defined as in the large parentheses of Eq. (3.29). The dashed line is for  $\gamma=0$ , the solid line is for  $\gamma=-0.10947$ , and the dotted line is  $-1/r$ .

(After adding this term, the formula is referred to as the modified local  $k_F$  formula in the following numerical comparisons.) Here,  $n^{1/2}(k)$  and  $n^{5/6}(k)$  are the Fourier transforms of  $n^{1/2}(r)$  and  $n^{5/6}(r)$ , and  $f(k/k_F)$  is a truncation function like  $\exp[-(k/2k_F)^2]$ . Note that this additional term does not affect the linear order, so the linear-response theory is still satisfied. The second term in (3.36) changes the original  $W_1(k)$  to  $W'_1(k)$  as

$$W'_1(k) = W_1(k) - \frac{8}{9} \left[ \frac{k}{k_F} \right]^2 f\left[ \frac{k}{k_F} \right]. \quad (3.37)$$

This new  $w'_1(r_0, r)$  can be computed in the same way as discussed above. One only needs to change the coefficients  $A_q$  of the Gaussian approximation. The first term in (3.36) changes the original von Weizsäcker term depending on  $k/k_F$ . For  $k < 2k_F$  it is the  $\frac{1}{9}$  von Weizsäcker term, while for  $k > 2k_F$  it is the full von Weizsäcker term. One can use the propagation method to compute  $f^{1/2}(k)n^{1/2}(k) \equiv d(k)$  in real space, then compute  $-\frac{8}{9}d(r)\nabla^2 d(r)$ . Actually, we compute  $f^{1/2}(k)n(k) \equiv n_1(k)$  first, then compute  $-\frac{8}{9}n_1^{1/2}(r)\nabla^2 n_1^{1/2}(r)$ . One Gaussian function is used for  $f^{1/2}(k)$ . Another method is to use a local truncation function depending on  $|\nabla n(r)|/n^{4/3}(r)$  to determine the factor in front of the von Weizsäcker term. There are many different truncation functions; a typical one is (see Ref. 17)

$$\exp\left[-\left[\frac{|\nabla n(r)|}{n^{4/3}(r)}\right]^2\right]. \quad (3.38)$$

However, as we found, all treatment of this modified von Weizsäcker term give qualitatively the same results. Here we only show the propagation treatment results in Tables IV–VI and Figs. 8 and 9. Note that, for  $1s^22s^22p^6$ , the shell structure is larger, and the correct amplitudes can almost be obtained. This is because, in the oscillating region, it is  $\frac{1}{9}$  the von Weizsäcker term. So the tendency to smooth the density is small, and the drive for oscillating from integral  $W'_1(r_0, r)$  is relatively large; as a result of the balance, the oscillation of the density is large. However, there are some drawbacks, including the Fermi energies, the tails, and the  $r=0$  densities. And the energy drops in column four of Tables IV–VI are usually larger than the original formula. This indicates some ambiguity of this modification, or, say, the lack of more deep guidelines. The existence of the  $n=3$  shell structure is still missing in the modified  $1s^22s^22p^63s^23p^63d^{10}$  density. But there is a small shoulder that corresponds to an  $n=3$  level. To see that, we changed the  $\sum_k W'_1(k)n^{5/6}(k)n^{5/6}(k)$  term in the modified formula to the local Thomas-Fermi term, and the resulting density is a structureless smooth curve, as shown in Fig. 9(b). The difference between this smooth density and the unchanged density demonstrates the effect of  $W'_1(k)$ . As one can see clearly, there is a shoulder around the place of the  $n=3$  level for the unchanged density, and there are three oscillations of the unchanged density around the changed smooth density that correspond to the three

shell structures.

There is a numerical problem we must mention here. In the tail region, because of the exponential decay of density  $n(r)$ , the  $b_{+1}$  will always get large no matter what grid we choose. As a result, we have to put  $b_{+1}$  equal to a constant (e.g., 0.15) after an  $r_c$  (but keep the relation between  $b_{+1}$ ,  $b_{-1}$ , and  $b_0$  correct). Fortunately,  $r_c$  is usually very large (outside the most interesting region) and this procedure is stable as long as we treat the values for  $r > r_c$  smoothly. But, for the  $1s^2$  system, the situation gets worse because the tail is relatively more important here. As a result, it is not known how well our numerical result represents the true solution. It appears that the major problem comes from the derivative term of  $G_\gamma(r, r')$  in Eq. (3.29). However, we can drop this term in Eq. (3.29) for the variational density. The linear order behaviors are the same. The drawback is that the kinetic-energy term in Eq. (3.29) is no longer a total derivative of a kinetic-energy functional. But it simplifies the equation. The results for other systems are similar to the above results. But for the  $2s^2$  system, this simplified formula gives a much better answer, very close to the exact one, as shown in Table IV and Fig. 7(b). Also note that, in column three of Tables IV–VI, for the variational density the total energies do not usually equal their kinetic energies; in other words, the virial theorem is not satisfied accurately. The scaling of the above kinetic-energy formula is correct, which means our formula (3.21) satisfied the following property:<sup>18</sup>

$$E_{\text{kin}}[n_\lambda] = \lambda^2 E_{\text{kin}}[n], \quad (3.39)$$

where  $n_\lambda(x, y, z) = \lambda^3 n(\lambda x, \lambda y, \lambda z)$ . As a result, the virial theorem should be satisfied (except the one just discussed above, which, without the derivative of  $G_\gamma$ , does not reach the true energy minimum). The lack of satisfaction of the virial theorem in Tables IV–VI measures the numerical accuracy in the solution. It might be caused by the fixing of  $b_{+1}$  (when  $r \rightarrow \infty$ ) mentioned above. It might also be caused by the finiteness of the grid, as indicated by the lack of satisfaction of the virial theorem by the variational densities of  $\text{TF}^{\frac{1}{3}}\text{W}$ . This lack of satisfaction of the virial theorem can be corrected by simply scaling the density. However, the modification is small.

In conclusion, this local dependence  $k_F$  formula can improve some aspects of the density in the solid systems. It can be applied to the isolated atoms, and gives variational densities with some shell structures. The attempts to improve the formula by adding an apparent second-order gradient expansion correction term have had some limited successes. Although all the variational densities of the above formulas show some shell structures, their

quantitative aspects vary depending on the detailed formulas, and they need to be improved. This also demonstrates the sensitivity of the variational densities to the kinetic-energy formula. To close this section, we would like to mention that complex Gaussian functions can be used in Eq. (3.4) [which corresponds to complex number  $b$  in (3.6)]. As a result, an accurate approximation of  $w_1$  in Eq. (3.4) and Fig. 6 can be achieved for several oscillations. And with this use of complex Gaussian functions, the local  $k_F$  method can also be applied to the second-order formulas in the next section.

#### IV. SECOND-ORDER FORMULAS

In the last section we discussed the dependence of  $k_F$  on local density  $n(r)$ . As shown before, it is very useful. However, it is only an intuitive treatment. If we want to know the detailed structure of the correction to formula (2.20), we need to go to the next order of perturbation theory. We will go back to use a constant  $k_F$  for simplicity, although the application of the techniques of the last section is still possible. The use of a constant  $k_F$  simplifies the computation, and the  $k_F$  dependence on  $n(r)$  is partially included in the second-order term. It is found in one dimension that the use of second order plus the use of a deformed mesh to include the local dependence of  $k_F$  can give rather good results. So second-order terms play a very important role in determining the density. The hope is that we can use such a finite-order formula (up to second-order, presumably) to determine the density to the chemical accuracy. This second-order theory should not be the direct second-order perturbation formula, which is rather poor. This theory is modified from the direct second-order formula. To do that, we must first find out the direct perturbation terms.

In real space, the plane-wave perturbation theory for density in all orders already exists:<sup>19</sup>

$$\gamma(r, r') = \sum_{j=0}^{\infty} \gamma_j(r, r'), \quad (4.1)$$

and

$$\gamma_j(r, r') = \frac{k_F^2}{2\pi^2} \int \prod_{l=1}^j \left[ \frac{-d^3 r_l V(r_l)}{2\pi} \right] \times j_l \left[ k_F \sum_{l=1}^{j+1} s_l \right] / \prod_{l=1}^{j+1} s_l. \quad (4.2)$$

Here  $\gamma(r, r')$  is the density matrix and

$$s_l = |r_l - r_{l-1}| \quad \text{and} \quad r_{j+1} = r', \quad r_0 = r.$$

For the second order, it is

$$n_2(r) = \gamma_2(r, r) = \frac{k_F^2}{2\pi^2} \int \frac{d^3 r_1}{2\pi} \frac{d^3 r_2}{2\pi} V(r_1) V(r_2) \frac{j_1(k_F |r - r_1| + k_F |r_1 - r_2| + k_F |r_2 - r|)}{|r - r_1| |r_1 - r_2| |r_2 - r|}. \quad (4.3)$$

Such double integrals are difficult in numerical computation. Our plan is to transform such integrals to  $k$  space; they then have the form

$$\sum_{k_1} \sum_{k_2} f(k_1, k_2) V(k_1) V(k_2).$$

For large  $k_1$  and  $k_2$ ,  $f(k_1, k_2)$  will go to zero. Thus the  $f(k_1, k_2)$  only occupies a finite region of scale  $k_F$  near the origin. Such  $f(k_1, k_2)$  can be broken down to a sum of several terms which have a form of  $f_1(k_1) f_2(k_2) f_3(k_1 + k_2)$ , thus the integral can be computed by the fast Fourier transform (FFT). This process is called the separation of the second-order term which will be discussed later in this section. Because we are most interested in the structure of the second order, a modestly approximated separation is enough. Such a separation has been proven to be not very difficult.

Now to change the integral into  $k$  space, we can directly Fourier transform Eq. (4.3). That probably can be done, but is not preferred by the authors. Rather, we chose the direct derivation from plane-wave perturbation. Let us assume the potential  $V(x)$  is small; first define

$$V(k) = \frac{1}{\Omega} \int V(x) e^{ikx} d^3x. \quad (4.4)$$

Here  $\Omega$  is the volume of the system. According to the perturbation theory, the perturbed wave functions are

$$\begin{aligned} \psi_k(x) = \frac{1}{\sqrt{\Omega}} \left[ e^{ikx} + \sum_{k_1} \frac{V(k-k_1)}{E_k - E_{k_1}} e^{ik_1x} \right. \\ \times \sum_{k_1, k_2} \frac{V(k_2 - k_1) V(k - k_2)}{(E_k - E_{k_1})(E_k - E_{k_2})} \\ \left. \times e^{ik_1x} \right]. \quad (4.5) \end{aligned}$$

Here  $E_k = \frac{1}{2}k^2$  is the plane-wave energy. So the total density is

$$\begin{aligned} n(x) &= \frac{2\Omega}{(2\pi)^3} \int_{k < k_F} d^3k \psi_k^*(x) \psi_k(x) \\ &= n_0 + n_1(x) + n_2(x). \quad (4.6) \end{aligned}$$

Substitute Eq. (4.5) in (4.6), and, after some change of index, we have

$$\begin{aligned} n_2(x) &= \frac{\pi}{k_F} \frac{2^3}{(2\pi)^3} \sum_{k_1} \sum_{k_2} \sum_{k_3} \delta_{k_1 + k_2 + k_3} V(k_1) \\ &\quad \times V(k_2) I(k_1, k_2, k_3) e^{ik_3x}. \quad (4.7) \end{aligned}$$

Here

$$I(k_1, k_2, k_3) = U(k_1, k_2) + U(k_1, k_3) + U(k_2, k_3) \quad (4.8)$$

and

$$\begin{aligned} U(k_1, k_2) &= \frac{\pi}{k_F} \\ &\quad \times \int_{k < k_F} d^3k \frac{1}{[k^2 - (k - k_1)^2][k^2 - (k + k_2)^2]}. \quad (4.9) \end{aligned}$$

Now we have a symmetry form for  $k_1$ ,  $k_2$ , and  $k_3$ . Our task is to find  $U(k_1, k_2)$ . Expanding the square in (4.9), we have

$$U(k_1, k_2) = \frac{\pi}{k_F} \frac{1}{k_1^2 k_2^2} \int_{k < k_F} d^3k \frac{1}{\mathbf{k} \cdot \mathbf{a}_1 - 1} \frac{1}{\mathbf{k} \cdot \mathbf{a}_2 - 1}, \quad (4.10)$$

with the definition

$$\mathbf{a}_1 = 2\mathbf{k}_1/k_1^2 \quad \text{and} \quad \mathbf{a}_2 = -2\mathbf{k}_2/k_2^2. \quad (4.11)$$

Now to carry out the integral  $\int d^3k$ , we used the well-known identity,

$$\frac{1}{ab} = \int_0^1 dx \frac{1}{[ax + b(1-x)]^2}. \quad (4.12)$$

Applied to the above Eq. (4.10), we have

$$U(k_1, k_2) = \frac{\pi}{k_F} \frac{1}{k_1^2 k_2^2} \int_0^1 dx \int_{k < k_F} d^3k \frac{1}{[\mathbf{k} \cdot \mathbf{b}(x) - 1]^2}, \quad (4.13)$$

with  $\mathbf{b}(x)$  defined as

$$\mathbf{b}(x) = \mathbf{a}_1 x + \mathbf{a}_2 (1-x). \quad (4.14)$$

The integral  $\int d^3k$  in Eq. (4.13) can be easily carried out, and then we have

$$\begin{aligned} U(k_1, k_2) &= \frac{\pi}{k_F} \frac{4\pi}{k_1^2 k_2^2} \left[ -k_F \int_0^1 dx \frac{1}{b^2} \right. \\ &\quad \left. + \frac{1}{2} \int_0^1 \frac{1}{b^3} \ln \left| \frac{k_F b + 1}{k_F b - 1} \right| dx \right]. \quad (4.15) \end{aligned}$$

Note that the above equation depends only on the magnitude of  $\mathbf{b}$ . From the definition, we have

$$\begin{aligned} b^2 &= a_1^2 x^2 + a_2^2 (1-x)^2 - 2a_1 a_2 x (1-x) \cos\theta \\ &= (a_1^2 + a_2^2 + 2a_1 a_2 \cos\theta) x^2 \\ &\quad - 2a_2 (a_2 + a_1 \cos\theta) x + a_2^2. \quad (4.16) \end{aligned}$$

Here  $\theta$  is the angle between  $\mathbf{k}_1$  and  $\mathbf{k}_2$ . Substituting this formula for  $b(x)$ , the integrals  $\int dx$  in Eq. (4.15) can be carried out by the conventional partial integral methods. The final result is, if  $k_3^2 - 4 \sin^2\theta \geq 0$ ,

$$U(k_1, k_2) = \frac{1}{4k_1 k_2 \sin^2 \theta} \left\{ (k_1 \cos \theta + k_2) \ln \left| \frac{2+k_1}{2-k_1} \right| + (k_2 \cos \theta + k_1) \ln \left| \frac{2+k_2}{2-k_2} \right| \right. \\ \left. + (k_3^2 - 4 \sin^2 \theta)^{1/2} \ln \left| \frac{(4 \cos \theta + k_1 k_2) - 2(k_3^2 - 4 \sin^2 \theta)^{1/2}}{(4 \cos \theta + k_1 k_2) + 2(k_3^2 - 4 \sin^2 \theta)^{1/2}} \right| \right\}, \quad (4.17)$$

and, if  $k_3^2 - 4 \sin^2 \theta \leq 0$ ,

$$U(k_1, k_2) = \frac{1}{4k_1 k_2 \sin^2 \theta} \left\{ (k_1 \cos \theta + k_2) \ln \left| \frac{2+k_1}{2-k_1} \right| + (k_2 \cos \theta + k_1) \ln \left| \frac{2+k_2}{2-k_2} \right| \right. \\ \left. - 2(4 \sin^2 \theta - k_3^2)^{1/2} \left[ \pi + \arctan \left( \frac{-2(4 \sin^2 \theta - k_3^2)^{1/2}}{k_1 k_2 + 4 \cos \theta} \right) \right] \right\}. \quad (4.18)$$

Note that, for reasons of simplicity, in the above formula  $k_1$  and  $k_2$  are renormalized by  $k_F$ , i.e., they are actually  $k_1/k_F$  and  $k_2/k_F$ . Although the formula falls into two regions with different forms, there is no discontinuity at the boundary. There is no physical significance for the boundary of the two regions. Also note that  $U(\mathbf{k}_1, \mathbf{k}_2)$  is only dependent on  $k_1$ ,  $k_2$ , and  $\theta$ , which is also a function of  $k_1$ ,  $k_2$ , and  $k_3$ , so  $U(\mathbf{k}_1, \mathbf{k}_2)$  and  $I(\mathbf{k}_1, \mathbf{k}_2, \mathbf{k}_3)$  are also only the functions of  $k_1$ ,  $k_2$ , and  $k_3$ . That must be true because of the overall rotational symmetry. So the function  $I(k_1, k_2, k_3)$  can be represented in a three-dimensional space with axes  $k_1$ ,  $k_2$ , and  $k_3$  and in a triangle cone:

$$k_1 + k_2 \geq k_3, \quad k_2 + k_3 \geq k_1, \quad k_1 + k_3 \geq k_2. \quad (4.19)$$

To separate  $I(k_1, k_2, k_3)$ , we only need to separate it in this variable space.

Now we have the density expressed in terms of the potential  $V(x)$ . What we want is the kinetic energy in terms of the density  $n(r)$ . As in the derivation of the gradient expansion, we can also compute the kinetic energy in the perturbation theory, then invert the  $V(r) \rightarrow n(r)$  relation and get the kinetic energy expressed by the density. However, here we will use another method, which first assumes a form for the kinetic energy based on the symmetry arguments. Then solving the Euler equation to get the variational density from the kinetic energy by requiring the resulting density to be equal to the above second-order formula of the density, we can get the kinetic-energy expression.

To get the second-order density, we need a third-order kinetic-energy functional:

$$T[n] = T_0 + \int \int \Delta n(x_1) \Delta n(x_2) f_1(x_1, x_2) d^3 x_1 d^3 x_2 \\ + \int \int \int \Delta n(x_1) \Delta n(x_2) \Delta n(x_3) \\ \times f_2(x_1, x_2, x_3) d^3 x_1 d^3 x_2 d^3 x_3. \quad (4.20)$$

From the translational symmetry, we have

$$f_1(x_1, x_2) = f_1(x_1 - x_2), \quad (4.21) \\ f_2(x_1, x_2, x_3) = f_2(x_1 - x_2, x_1 - x_3).$$

After solving the Euler equation

$$\frac{\delta}{\delta n} \left[ T[n] + \int \Delta V(x) n(x) d^3 x + \int \lambda n(x) d^3 x \right] = 0, \quad (4.22)$$

we have

$$\frac{\delta T_0}{\delta n} + \lambda + 2 \int f_1(x - x_1) \Delta n(x_1) d^3 x_1 \\ + 3 \int \Delta n(x_1) \Delta n(x_2) f_2(x, x_1, x_2) d^3 x_1 d^3 x_2 \\ + \Delta V(x) = 0. \quad (4.23)$$

Using the Fourier transforms

$$\Delta V(k) = \frac{1}{\Omega} \int \Delta V(x) e^{ikx} d^3 x, \quad (4.24) \\ \Delta n(k) = \frac{1}{\Omega} \int \Delta n(x) e^{ikx} d^3 x,$$

we have

$$\Delta V(k) + 2 f_1(k) \Delta n(k) \\ + 3 \sum_{k_1} \sum_{k_2} \delta_{k+k_1+k_2} \Delta n(k_1) \Delta n(k_2) f_2(k_1, k_2) \\ + \left[ \frac{\delta T_0}{\delta n} + \lambda \right] \delta_{k,0} = 0. \quad (4.25)$$

Here

$$f_1(k) = \int f_1(x) e^{ikx} d^3 x$$

and

$$f_2(k_1, k_2) = \int \int f_2(x_1 - x_3, x_2 - x_3) \\ \times e^{ik_1(x_1 - x_3)} e^{ik_2(x_2 - x_3)} \\ \times d^3(x_1 - x_3) d^3(x_2 - x_3). \quad (4.26)$$

Now, substituting the  $\Delta n(k)$  expression in Eq. (4.7) into Eq. (4.25) and setting equal the two sides of the equation order by order, we have

$$f_1(k) = \frac{1}{2f(k)} = \frac{(3\pi^2)^{2/3}}{6n_0^{1/3}} W^{-1}(k), \quad (4.27)$$

$$\begin{aligned} f_2(k, k_1, k_2) &= -\frac{1}{3\pi^2 k_F} f^{-1}(k) f^{-1}(k_1) \\ &\quad \times f^{-1}(k_2) I(k, k_1, k_2) \\ &= -\frac{\pi^2}{9n_0 k_F} W^{-1}(k) W^{-1}(k_1) \\ &\quad \times W^{-1}(k_2) I(k, k_1, k_2). \end{aligned} \quad (4.28)$$

Here

$$W(q) = \frac{1}{2} + \frac{q^2 - 4}{8q} \ln \left| \frac{2-q}{2+q} \right|. \quad (4.29)$$

The  $k$ ,  $k_1$ , and  $k_2$  in the above formula have been renormalized by  $1/k_F$  as before, and  $I(k, k_1, k_2)$  is given by (4.8).

Now we have a perturbation formula for kinetic energy in terms of density. Following Sec. II, we want to express our first two orders of kinetic energy based on the formulas in Sec. II. For that purpose, we write down our kinetic-energy functional as

$$\begin{aligned} T[n] &= a_{11} \int \int n^{5/6}(r_1) W_1(r_1 - r_2) n^{5/6}(r_2) d^3 r_1 d^3 r_2 - b_{11} \int n^{5/3}(r) d^3 r - \frac{1}{2} \int n^{1/2}(r) \nabla^2 n^{1/2}(r) d^3 r \\ &\quad + \int \int \int \Delta n(r_1) \Delta n(r_2) \Delta n(r_3) \Pi(r_1, r_2, r_3) d^3 r_1 d^3 r_2 d^3 r_3. \end{aligned} \quad (4.30)$$

The  $a_{11}$ ,  $b_{11}$  and  $W_1$  are given in Sec. II. Now we must determine what is  $\Pi(r_1, r_2, r_3)$ . To find out, we express  $n(r)$  as  $n_0 + \Delta n(r)$ , and then substitute it in the above formula. We get some left-out third order from the first three terms, and, through comparison with the direct perturbation formula (4.20), we get

$$\begin{aligned} \Pi(k_1, k_2, k_3) &= f_2(k_1, k_2, k_3) - (3\pi^2)^{2/3} n_0^{-4/3} \left[ -\frac{2}{45} W_1(k_3) + \frac{7}{270} - \frac{1}{16} k_3^2 \right] \\ &= -n_0^{-4/3} (3\pi^2)^{2/3} \left[ \frac{1}{27} W^{-1}(k_1) W^{-1}(k_2) W^{-1}(k_3) I(k_1, k_2, k_3) - \frac{2}{45} W_1(k_3) + \frac{7}{270} - \frac{1}{16} k_3^2 \right]. \end{aligned} \quad (4.31)$$

Because  $k_1$ ,  $k_2$ , and  $k_3$  are symmetrized in the integral, we can symmetrize this formula and get

$$\begin{aligned} \Pi(k_1, k_2, k_3) &= -n_0^{-4/3} (3\pi^2)^{2/3} \left[ \frac{1}{27} W^{-1}(k_1) W^{-1}(k_2) W^{-1}(k_3) I(k_1, k_2, k_3) \right. \\ &\quad \left. - \frac{1}{108} W^{-1}(k_1) - \frac{1}{108} W^{-1}(k_2) - \frac{1}{108} W^{-1}(k_3) - \frac{1}{72} k_1^2 - \frac{1}{72} k_2^2 - \frac{1}{72} k_3^2 + \frac{1}{108} \right]. \end{aligned} \quad (4.32)$$

Now we discuss some properties of  $\Pi(k_1, k_2, k_3)$ . First, as  $k_1, k_2, k_3 \rightarrow 0$ ,

$$\Pi(k_1, k_2, k_3) \rightarrow 0.$$

This is because we have included the Thomas-Fermi theory in the first two orders of the formula. Because the TF theory is the result of all order summations of perturbation theory (4.2),<sup>20</sup> all higher-order corrections in our formula must be zero near the  $k=0$  origin. This is significant, because most contributions usually come from the small- $k$  region, and now they are all absent for higher-order corrections. For example, the third-order correction in Eq. (4.30) is found to be only one tenth of the original third-order contribution in Eq. (4.20), in the system we studied. This obviously speeds up the convergence of our formula.

Next, as  $k_1, k_2, k_3 \rightarrow \infty$ ,

$$\Pi(k_1, k_2, k_3) \rightarrow \text{finite}, \quad (4.33)$$

unlike the original second-order term  $f_2(k_1, k_2, k_3)$ , which scales as  $k^2$ . This is because we included  $-\frac{1}{2} n^{1/2} \nabla^2 n^{1/2}$  in the first two orders of our formula. This further confirms the conjecture that the full von Weizsäcker term is the correct limit for  $k \rightarrow \infty$ . So the third order and all the higher orders will no longer have such  $k^2$  scaling. They can only have lower power scaling on  $k$ .

Note that there is an overall  $n_0^{-4/3}$  dependence on  $\Pi(k_1, k_2, k_3)$ . In the spirit of all our procedures discussed previously, we absorb this overall dependence in  $\Delta n(k_1) \Delta n(k_2) \Delta n(k_3)$ . So we define  $\Pi_1$  as

$$\Pi_1(k_1, k_2, k_3) = (3\pi^2)^{-2/3} n_0^{4/3} \Pi(k_1, k_2, k_3). \quad (4.34)$$

Then

$$\begin{aligned} T[n] &= a_{11} \int \int n^{5/6}(r_1) W_1(r_1 - r_2) n^{5/6}(r_2) d^3 r_1 d^3 r_2 - b_{11} \int n^{5/3}(r) d^3 r - \frac{1}{2} \int n^{1/2}(r) \nabla^2 n^{1/2}(r) d^3 r \\ &\quad + \left(\frac{9}{5}\right)^3 (3\pi^2)^{2/3} \int \int \int \Delta n^{5/9}(r_1) \Delta n^{5/9}(r_2) \Delta n^{5/9}(r_3) \Pi_1(r_1, r_2, r_3) d^3 r_1 d^3 r_2 d^3 r_3. \end{aligned} \quad (4.35)$$

(This will be referred to as the second-order formula in the following numerical comparisons.) Note that here  $\Delta n^{5/9}(r) = n^{5/9}(r) - (n^{5/9})_{\text{av}}$ .

From the expression of  $\Pi(k_1, k_2, k_3)$ , we find that as  $k_1, k_2, k_3 \rightarrow \infty$ ,

$$\begin{aligned} \Pi_1(k_1, k_2, k_3) \rightarrow & -\frac{13}{540} - \frac{1}{120} \left[ \left( \frac{k_1^2}{k_2 k_3} \right)^2 + \left( \frac{k_2^2}{k_1 k_3} \right)^2 + \left( \frac{k_3^2}{k_1 k_2} \right)^2 \right. \\ & \left. - \left( \frac{k_2}{k_1} \right)^2 - \left( \frac{k_1}{k_2} \right)^2 - \left( \frac{k_2}{k_3} \right)^2 - \left( \frac{k_3}{k_2} \right)^2 - \left( \frac{k_1}{k_3} \right)^2 - \left( \frac{k_3}{k_1} \right)^2 \right]. \end{aligned} \quad (4.36)$$

Another feature of  $\Pi_1(k_1, k_2, k_3)$  is that when  $k_1, k_2$ , or  $k_3$  crosses 2, it diverges to infinity as  $\ln|(2-k)/(2+k)|$ . Fortunately, the integral of such a divergent area is finite. This means that a perturbation theory with continuous spectrum  $n(k)$  will not have divergent second-order results from the formula. Then, in practice, it is reasonable to replace the infinite peak with a smooth finite one, but keep the integral of the peaks the same. We found that the system is not very sensitive to this procedure.

Now let us discuss the separation of the second order. To efficiently compute the second order, we proposed to separate  $\Pi_1(k_1, k_2, k_3)$  into a sum of several terms, with each term a product of  $f_1(k_1)f_2(k_2)f_3(k_3)$ . Then it can be computed by the FFT. In principle, any function  $\Pi_1(k_1, k_2, k_3)$  can be decomposed in this way. The question is how to minimize the number of terms in the separation. First, we know  $\Pi_1$  is only a function of  $k_1, k_2$ , and  $k_3$  and is defined in the triangle cone. So we only need to consider the separation in that region. Because the function  $\Pi_1(k_1, k_2, k_3)$  has a rotational symmetry about 1, 2, and 3, its separation terms must also have such symmetry. To separate  $\Pi_1$  effectively, we must first have an understanding of its structure in the space, and then decide what kind of terms we need to use. Unlike  $I(k_1, k_2, k_3)$ ,  $\Pi_1$  has a finite tail for  $k \rightarrow \infty$ . Fortunately,

the analytical form for that region is available. We need a big term  $ccc_1$  [which includes several small terms like  $f_1(k_1)f_2(k_2)f_3(k_3)$ ] to describe that region. Then what is left is an isolated region in the scale of  $k_F$  near the origin. The biggest feature for the left value is a wall-like structure for  $k_1=2k_F$  and  $k_2=2k_F$  and  $k_3=2k_F$ . For  $k_1, k_2, k_3 \leq 2k_F$ , it is negative. When  $k$  crosses  $2k_F$ , the value abruptly jumps to a positive value and then falls down. We need one big term  $ccc_2$  to describe the  $k \leq 2k_F$  negative region, and another term  $ccc_3$  to describe the left wall. Finally, another term  $ccc_4$  is needed to modify the final structure near the edge of the walls. We found out that these four big terms are enough to describe  $\Pi_1$  reasonably well. These four big terms are constructed by hand with the help of computer visualization. They are created one after another, and no optimizations are performed, although that might significantly improve the accuracy. What we want to show is that even such a primitive approximation can give good results. In the following, we write down these four big terms.

The first big term is

$$ccc_1 = \Gamma(k_1, k_2, k_3) f_1(k_1) f_1(k_2) f_1(k_3), \quad (4.37)$$

and

$$\begin{aligned} \Gamma(k_1, k_2, k_3) = & -\frac{13}{540} - \frac{1}{120} \left[ \left( \frac{k_1^2}{k_2 k_3} \right)^2 + \left( \frac{k_2^2}{k_1 k_3} \right)^2 + \left( \frac{k_3^2}{k_1 k_2} \right)^2 \right. \\ & \left. - \left( \frac{k_2}{k_1} \right)^2 - \left( \frac{k_1}{k_2} \right)^2 - \left( \frac{k_2}{k_3} \right)^2 - \left( \frac{k_3}{k_2} \right)^2 - \left( \frac{k_1}{k_3} \right)^2 - \left( \frac{k_3}{k_1} \right)^2 \right], \end{aligned} \quad (4.38)$$

and the  $f_1(k)$  is defined as

$$f_1(k) = 0.4k^2 \frac{1}{1 + \left( \frac{k}{2.33} \right)^{10}} \quad \text{when } k \leq 1.95, \quad (4.39)$$

$$f_1(k) = \frac{0.06}{(k - 1.835)^{0.75}} + 0.05(k - 1.8)e^{-2.5(k-2)} + 1$$

when  $k \geq 1.95$ .

Note that, in the above and in the following formulas, all  $k$  are actually  $k/k_F$ .

The second big term is

$$ccc_2 = [f_3(k_1) + f_3(k_2) + f_3(k_3)] f_2(k_1) f_2(k_2) f_2(k_3). \quad (4.40)$$

Here

$$f_2(k) = 0.5 + \frac{k^2 - 4}{8k} \ln \left| \frac{2-k}{2+k} \right|, \quad (4.41)$$

and  $f_3(k)$  is

$$f_3(k) = \begin{cases} \frac{(-\frac{1}{81}k^2 - 0.002k^4)}{1 + \left[\frac{k}{1.955}\right]^{28}} & \text{when } k \leq 1.84 \\ -0.055e^{-4.2(k-1.84)} & \text{when } k \geq 1.84. \end{cases} \quad (4.42)$$

The third big term is

$$ccc_3 = f_4(k_2)f_4(k_3)f_5(k_1) + f_4(k_1)f_4(k_3)f_5(k_2) + f_4(k_1)f_4(k_2)f_5(k_3). \quad (4.43)$$

Here

$$f_4(k) = \begin{cases} 1 & \text{for } k \leq 2 \\ e^{-3(k-2)} & \text{for } k \geq 2, \end{cases} \quad (4.44)$$

and

$$f_5(k) = \begin{cases} 0.02e^{-30(k-2.15)^2} & \text{for } k \leq 2.15 \\ 0.02e^{-1.8(k-2.15)^2} & \text{for } k \geq 2.15. \end{cases} \quad (4.45)$$

The fourth big term is

$$ccc_4 = -0.017[f_6(k_1)f_7(k_2)f_7(k_3) + f_6(k_2)f_7(k_1)f_7(k_3) + f_6(k_3)f_7(k_1)f_7(k_2)]. \quad (4.46)$$

Here

$$f_6(k) = e^{-(k-3)^2} \quad (4.47)$$

and

$$f_7(k) = \begin{cases} 0 & \text{for } k \leq 0.7 \\ \frac{1}{1.25}(k-1.95)+1 & \text{for } 0.7 \leq k \leq 1.95 \\ e^{-2(k-1.95)} & \text{for } k \geq 1.95. \end{cases} \quad (4.48)$$

The contour plots of  $\Pi_1$  and its separated form in one cross section are given in Fig. 11. It can be seen that, although the separation is not absolutely accurate, it preserves the basic structure of the original function  $\Pi_1$ .

Finally, let us discuss how many FFT's are needed to compute the second order in the above separated form. Because the symmetry is of above form, the required number of FFT's is far less than it appears to be. First, to compute the total kinetic energy, we have

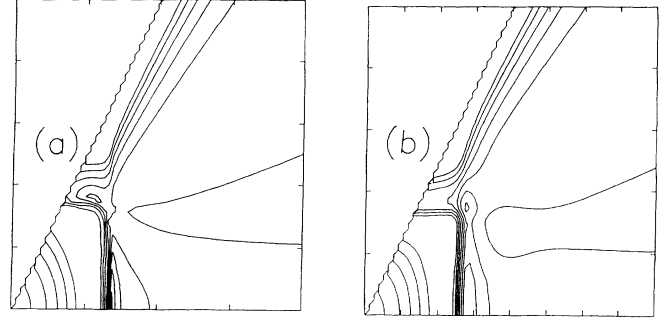


FIG. 11. Comparison of exact (a) and separated (b)  $\Pi_1(k_1, k_2, k_3)$ . The contour plots are on the [110] plane of  $(k_1, k_2, k_3)$  space.

$$T_2[n] = \sum_{k_1, k_2, k_3} \delta_{k_1+k_2+k_3} \Pi_1(k_1, k_2, k_3) \times \Delta n^{5/9}(k_1) \Delta n^{5/9}(k_2) \Delta n^{5/9}(k_3). \quad (4.49)$$

Here as before,  $\Delta n^{5/9}(k)$  should be understood as the Fourier transform of  $\Delta n^{5/9}(r)$ . If we start with a known  $\Delta n^{5/9}(k)$ , then we need five FFT's to compute  $ccc_1$ , and two FFT's for each of  $ccc_2$ ,  $ccc_3$ , and  $ccc_4$ . So the total number of FFT's is 11. To solve the variational density, we need to compute the following expression in the Euler equation:

$$\sum_{k_1, k_2, k_3} \delta_{k_1+k_2+k_3} \Pi_1(k_1, k_2, k_3) \Delta n^{5/9}(k_2) \Delta n^{5/9}(k_3). \quad (4.50)$$

Because of the loss of some symmetry, this computation is more involved. The number of FFT's to compute this expression is ten for  $ccc_1$ , and four for each of  $ccc_2$ ,  $ccc_3$ , and  $ccc_4$ . So the total number is 22. Twenty-two FFT computations is practical, and is much less than the all-wave-function computations of the Kohn-Sham equation. But it is still much larger than the other part of computation in the Euler equation for the density  $n(r)$ , which has only five or six FFT's for the first-order and potential computations. However, in the iterative computation of the Euler equation,<sup>21</sup> because the second-order term is only a small modification of the first-order and potential terms, it does not control the size of the convergent step  $\Delta t$ . As a result, we only need to update the second-order term every few (three or four) steps. Then the computation time spent on the second order can be the same as or even less than the first order and potential terms.

Before we go into numerical application, we will first modify our formula one step further, as we did at the end of the last section. So far, the formula includes the first and second order of perturbation theory, and it also includes the Thomas-Fermi theory. The TF theory is the first term in the gradient expansion series, so we are in a position to combine the gradient expansion and perturbation theories. We can incorporate the second-order gradient expansion term by adding a term similar to that at the end of the last section:

$$T_{\text{add}} = -\left(\frac{8}{9}\right)^{\frac{1}{2}} \sum_k \left[ n^{1/2}(k) k^2 f_8(k) n^{1/2}(k) - \left(\frac{3}{5}\right)^2 \frac{1}{n^{2/3}} n^{5/6}(k) k^2 f_8(k) n^{5/6}(k) \right]. \quad (4.51)$$

Here  $n^{1/2}(k)$  and  $n^{5/6}(k)$  are the Fourier transforms of  $n^{1/2}(r)$  and  $n^{5/6}(r)$ , respectively, and  $f_8(k)$  is a truncation function like  $[1+(k/2)^{10}]^{-1}$ , which equals 1 when  $k \rightarrow 0$  and goes to zero when  $k \gg 2$ . When such a term is added to the first-order formula (2.20), we do see an improvement for the variational density  $n(r)$ , especially for small- $k$  components. When this additional term is used for the second-order formula, the second-order term should be modified as

$$\Pi_2(k_1, k_2, k_3) = \Pi_1(k_1, k_2, k_3) + \frac{1}{81} [k_1^2 f_8(k_1) + k_2^2 f_8(k_2) + k_3^2 f_8(k_3)]. \quad (4.52)$$

As expected,  $\Pi_2 \rightarrow k^4$  when  $k \rightarrow 0$ . Unfortunately, there are big tails for  $k_1 \sim k_F$  and  $k_2, k_3 \rightarrow \infty$  and its symmetrized counterparts. These big tails give too much of a contribution and cause a large second-order term. The resulting variational density gets worse. As a rule of thumb, to get a better convergent result, we need to get smaller higher-order terms. So the increase of the second-order value is not a good sign, unless we do not include the second-order term. To control the situation, we have found that a different additional term can be applied:

$$T_{\text{add}} = -\left(\frac{8}{9}\right)^{\frac{1}{2}} \sum_k \left[ n_1^{1/2}(k) k^2 f_8(k) n_1^{1/2}(k) - \left(\frac{3}{5}\right)^2 \frac{1}{n_0^{2/3}} n_1^{5/6}(k) k^2 f_8(k) n_1^{5/6}(k) \right]. \quad (4.53)$$

Here, as before,  $n_1^{1/2}(k)$  and  $n_1^{5/6}(k)$  are the Fourier transforms of  $n_1^{1/2}(r)$  and  $n_1^{5/6}(r)$ , respectively. Here another truncation function is applied to  $n(k)$  as

$$n_1(k) = n(k) f_9(k). \quad (4.54)$$

Under this additional term, the modified second order is

$$\Pi_2(k_1, k_2, k_3) = \Pi_1(k_1, k_2, k_3) + \frac{1}{81} [k_1^2 f_8(k_1) + k_2^2 f_8(k_2) + k_3^2 f_8(k_3)] \times f_9(k_1) f_9(k_2) f_9(k_3). \quad (4.55)$$

We used  $[1+(k/2)^{10}]^{-1}$  for  $f_8(k)$  and  $e^{-\lambda(k/2)^2}$  for  $f_9(k)$ .  $\lambda=1$  is used in the following computations. Thus there is no large tail for  $\Pi_2(k_1, k_2, k_3)$ . This modified second-order formula does give better results than the original second-order formula. Then we have a formula that includes the second-order gradient expansion and

second-order perturbation theory. This final formula [Eq. (4.35), with  $\Pi_1$  replaced by  $\Pi_2$  in Eq. (4.55) plus  $T_{\text{add}}$  of Eq. (4.53)] will be used in the following numerical study.

The same silicon is used in diamond-structure systems. The energy results are in Tables I–III. The kinetic energies computed by the correct densities are better than the  $\text{TF}_5^{\perp}\text{W}$  results. The typical components for the second-order formula kinetic energy are (for the second system) 8.7233 for the  $W_1$  integral term, 3.3221 for the von Weizsäcker term,  $-0.1506$  for the second-order term, and  $-0.0583$  for the above  $T_{\text{add}}$  term (all in hartree). So the second-order term and the  $T_{\text{add}}$  term are indeed small. For the variational density, the energy drops are further reduced from the first-order results. The density contour plots for the second-order formula are shown in Figs. 4(d), 4(e), and 5(c). The errors of variational densities are reduced by a factor of 2 from the first-order formula, and by a factor of 4 from the  $\text{TF}_5^{\perp}\text{W}$  results. Most importantly, it increased the bond charges, and the amplitudes are almost right. However, the results do crucially depend on the pseudopotentials. For the second pseudopotential, which is smooth, the situation is much better than the first one. One can estimate how good the current formula is for a given pseudopotential by comparing it with our two examples. That is one of the reasons why we computed two pseudopotential systems in this paper.

Now let us check the quality of the separation scheme. Because of the symmetry of the diamond structure, the second-order term can be computed directly without too much difficulty. Using the  $V_{\text{tot}}$  in Fig. 3(b), the variation-

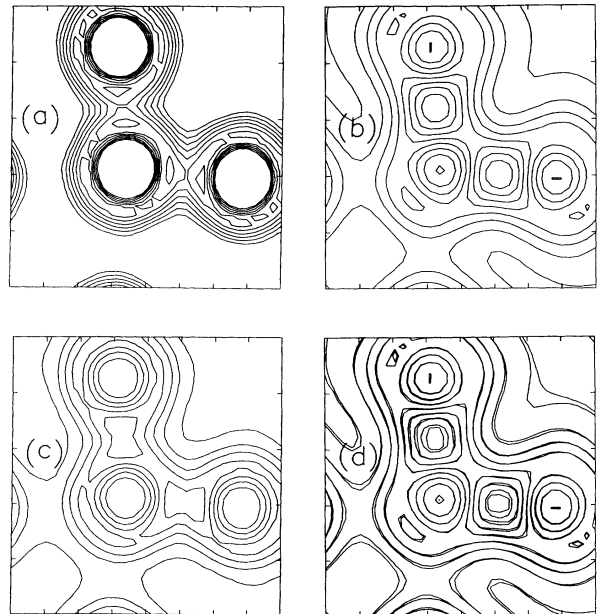


FIG. 12. A silicon amorphous example. (a) Total potential, (b) Kohn-Sham exact density, (c)  $\text{TF}_5^{\perp}\text{W}$  density, (d) second-order formula variational density compared with the exact Kohn-Sham density.

al density of the separated formula is compared with the unseparated exact second-order formula density. The difference between these two densities is 1.6% according to Eq. (2.10). The error of the separated formula density is 6.0% comparing to 5.5% of the exact second-order formula result. So, as we can see, the separation is good enough to preserve the usefulness of the second-order term.

Another question is whether the high symmetry in the diamond structure somehow effects our numerical results thus limiting our conclusions. To answer this question, we computed a 12-silicon-atom amorphous system.<sup>22</sup> The results are shown in Fig. 12 compared with the exact density and the  $TF_{\frac{1}{2}}W$  density. As we can see, the same conclusion can be obtained, including the accuracy of the density, the bond charge, etc. So our results do not depend on the symmetry of the diamond structure; they are general.

In conclusion, the second-order formula does improve the kinetic energy and variational density further from

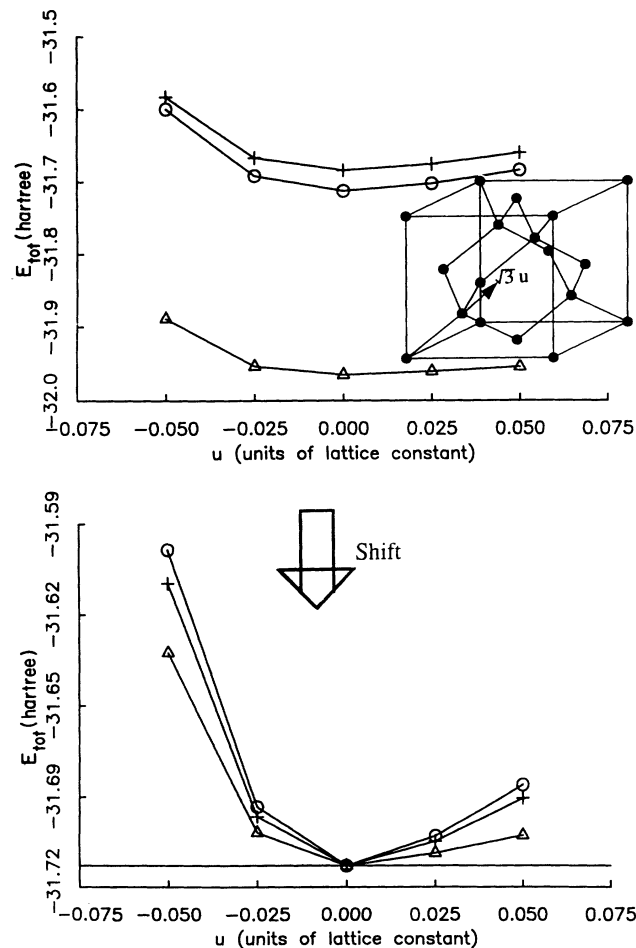


FIG. 13. Total energy vs atomic position. Values are in a.u. The  $x$  axis is  $u/\sqrt{3}$ . Note that 0.25 is the equilibrium position. The lower graph is the result after putting the three curves together. Only one atom is moved in the eight atom cell.  $\circ$ , Kohn-Sham results;  $+$ , current formula results;  $\triangle$ ,  $TF_{\frac{1}{2}}W$  results.

the first-order formula. It gives good variational densities for smooth potentials.

## V. APPLICATIONS

We have put our emphasis on the variational densities and their contour plots. This is the right approach to study the formula, because the density itself provides the richest information and is also very sensitive to the kinetic-energy formula. However, from the application point of view, the more interesting things are the real chemical values computed by the current formula, including the cohesive energy, the forces on the atoms, and structural stabilities. They will allow us to determine how applicable the current formula is.

To compute the chemical values, we used the first pseudopotential defined by Eq. (2.21). This time the self-consistent computations are carried out. The densities are very similar to the non-self-consistent computations in the previous sections. Here what we emphasize are the total energies. We changed the atomic position in different ways, and looked at the energy curves. The

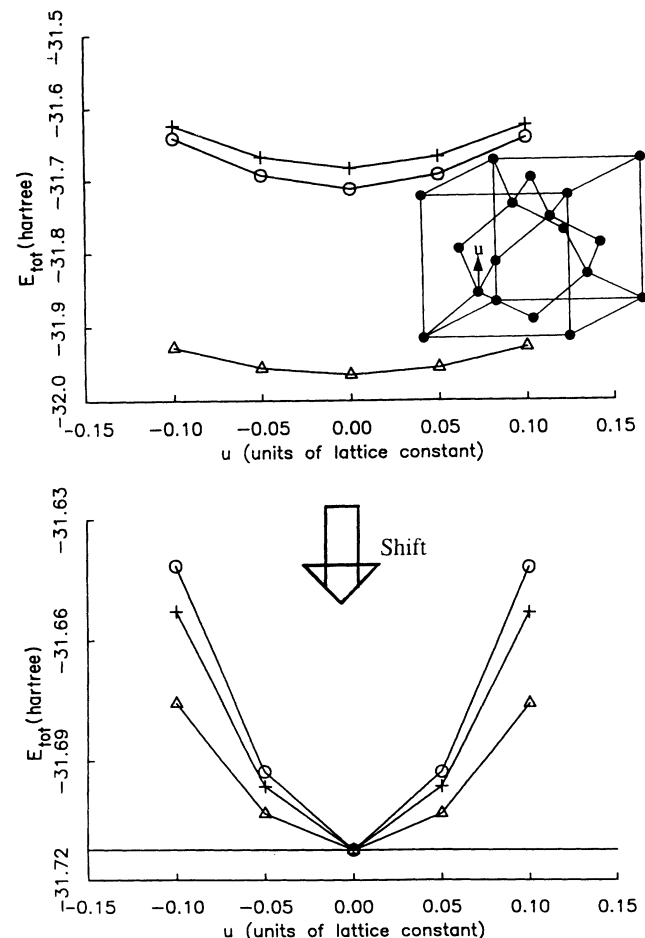


FIG. 14. Total energy vs atomic position. The  $x$  axis is  $u$  and 0.25 is the equilibrium position. Only one atom is moved in the eight atom cell.  $\circ$ , Kohn-Sham results;  $+$ , current formula results;  $\triangle$ ,  $TF_{\frac{1}{2}}W$  results.

Kohn-Sham results are compared with the current formula results and the  $TF_{\frac{1}{5}}W$  results. The latter results represent the best results among the previous existing formulas. Most of the results are shown in graphic form in Figs. 13–15. The improvement of current results over the  $TF_{\frac{1}{5}}W$  results is well seen. First, the cohesive energy is the energy difference between the solid configuration and the separated atoms. Because there is no convenient way to compute the isolated atoms by the current second-order formula, we will use the Kohn-Sham atomic energy to do that. If we assume that the Kohn-Sham result gives almost the correct binding energy, then, computed that way, the cohesive energies per atom for the Kohn-Sham current formula and the  $TF_{\frac{1}{5}}W$  result are 4.63, 3.85, and 11.50 eV. So the current formula results are more close to the Kohn-Sham result, and are much better than the  $TF_{\frac{1}{5}}W$  result. The forces of the atoms are all represented by the total energy versus atomic position curves. The current formula results are about 15–20% from the Kohn-Sham results. On the other hand, the

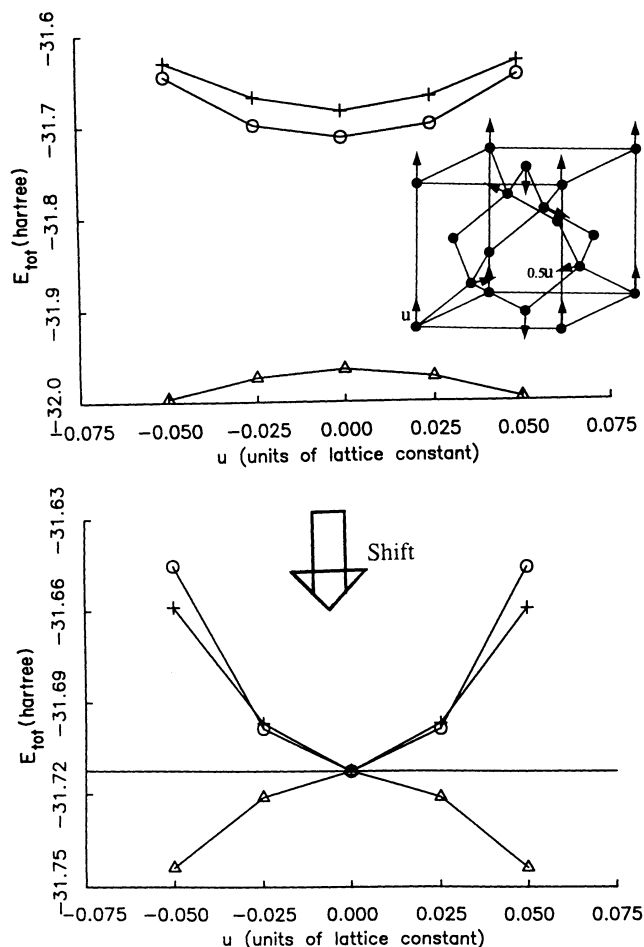


FIG. 15. Total energy vs atomic position. The x axis is  $u$ . Note that in the first order, the bond lengths are preserved.  $\circ$ , Kohn-Sham results;  $+$ , current formula results;  $\triangle$ ,  $TF_{\frac{1}{5}}W$  results. Note the instability of the  $TF_{\frac{1}{5}}W$  results against this displacement.

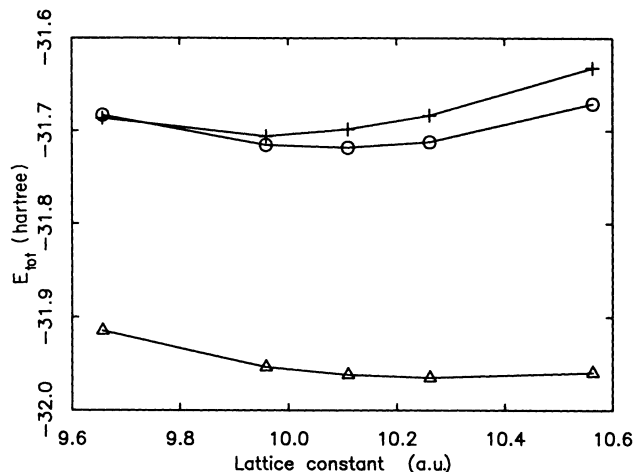


FIG. 16. Total energy vs lattice length. The x axis is the lattice length. The y axis is the total energy.  $\circ$ , Kohn-Sham results;  $+$ , current formula results;  $\triangle$ ,  $TF_{\frac{1}{5}}W$  results. Note the inclination of the current formula curve.

$TF_{\frac{1}{5}}W$  results are off by more than a factor of 2. Most interestingly, when the atoms moved transversely (so the bond lengths are conserved), the  $TF_{\frac{1}{5}}W$  is not stable (in Fig. 15, the curvature for the  $TF_{\frac{1}{5}}W$  energy curve is negative), while the current formula does give a stable result. So the current formula begins to give chemically correct answers. That is very significant, because all of the previous kinetic-energy functionals fail to do that.

Another value is the lattice length. The energy versus the lattice length are shown in Fig. 16. Although the current result is very close to the Kohn-Sham result, one problem is that the curve leans towards one side. This is because of the perturbative nature in our formula, especially the  $\Delta n^{5/9}$  term in the formula. So when the lattice length gets larger, the accuracy of the formula is better, and there is a systematic inclination of the curve. This is expected to be improved in future modifications of the formula. The bulk moduli for the Kohn-Sham current formula and  $TF_{\frac{1}{5}}W$  result are 1.24, 1.05, and 0.73 Mbar. Note that the current formula bulk modulus is better than the  $TF_{\frac{1}{5}}W$  bulk modulus, because the systematic error discussed above does not affect the bulk modulus as long as it is linear.

## VI. CONCLUSION

In this paper, we have presented a new kinetic-energy functional that is based on an integral term and its higher-order corrections, which replace the original Thomas-Fermi term. The second-order formula also incorporates the second-order gradient expansion formula. Because of the full von Weizsäcker term in the current formula, the rigorous cusp conditions for the electron density at the nucleus are satisfied. The current formula variational densities are much improved from the  $TF_{\frac{1}{5}}W$

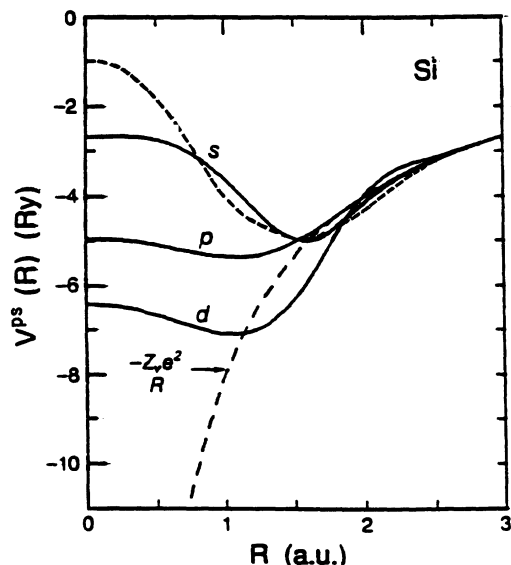


FIG. 17. The smoothness comparison of the currently used pseudopotential (dashed line) with the *ab initio* nonlocal pseudopotential (Ref. 23) (solid lines).

results, which represent the best results from the previously existing kinetic-energy functionals. Most importantly, the current variational densities give quantum-interference effects (shell structures) by using a kinetic-

energy functional in a real physical system. For a reasonably smooth potential, the formula gives quantitatively reasonable results, although to get chemical accuracy one further step of improvement is needed. We emphasized the application to solids instead of atoms. The solid system is where a kinetic-energy functional is needed most, and also where the current formula works best. To get good results, we currently need smooth pseudopotentials. The first pseudopotential we used for silicon is a realistic pseudopotential. The *ab initio* nonlocal pseudopotential, which works well for the Kohn-Sham approach, can have the same order of variation as this one [see Fig. 17 (Ref. 23)]. So if the current formula had worked for nonlocal pseudopotentials, it could give *ab initio* results with the same order of accuracy as we showed above. The challenge is how to make the formula work for nonlocal pseudopotentials. Besides, it could be possible to derive pseudopotentials directly from the current kinetic-energy formula. Such an approach has been proved to be useful.<sup>24</sup>

#### ACKNOWLEDGMENTS

We acknowledge useful discussions with Professor Mel Levy concerning the inherently correct scaling behavior of the functionals.

<sup>1</sup>For a review, see R. M. Dreizler and E. K. U. Gross, *Density Functional Theory: An Approach to the Quantum Many Body Problem* (Springer-Verlag, Berlin, 1990); in *The Single Particle Density in Physics and Chemistry*, edited by N. H. March and B. M. Deb (Academic, San Diego, 1987).  
<sup>2</sup>L. H. Thomas, Proc. Cambridge Philos. Soc. **23**, 542 (1926); E. Fermi, Z. Phys. **48**, 73 (1928).  
<sup>3</sup>E. Teller, Rev. Mod. Phys. **34**, 627 (1962).  
<sup>4</sup>C. F. von Weizsäcker, Z. Phys. **96**, 431 (1935).  
<sup>5</sup>D. A. Kirzhnits, Zh. Eksp. Teor. Fiz. **32**, 115 (1957) [Sov. Phys.—JETP **5**, 64 (1957)].  
<sup>6</sup>K. Yonei and Y. Tomishima, J. Phys. Soc. Jpn. **20**, 1051 (1965).  
<sup>7</sup>R. M. Dreizler and E. K. U. Gross, *Density Functional Theory: An Approach to the Quantum Many Body Problem* (Ref. 1), p. 133, Table 5.7.  
<sup>8</sup>R. M. Dreizler and E. K. U. Gross, *Density Functional Theory: An Approach to the Quantum Many Body Problem* (Ref. 1), pp. 102 and 98; J. P. Perdew, M. Levy, G. S. Painter, S. Wei, and J. B. Lagowski, Phys. Rev. B **37**, 838 (1988); W. Stich, E. K. U. Gross, P. Malzacher, and R. M. Dreizler, Z. Phys. A **309**, 5 (1982).  
<sup>9</sup>O. Gunnarsson, M. Jonson, and B. I. Lundqvist, Phys. Rev. B **20**, 3136 (1979); P. Tarazona, Phys. Rev. A **31**, 2672 (1985); W. A. Curtin and N. W. Ashcroft, *ibid.* **32**, 2909 (1985).

<sup>10</sup>P. Hohenberg and W. Kohn, Phys. Rev. **136**, B864 (1964).  
<sup>11</sup>M. L. Plumer and D. J. W. Geldart, J. Phys. C **16**, 677 (1983).  
<sup>12</sup>C. Herring, Phys. Rev. A **34**, 2614 (1986); C. Herring and M. Chopra, *ibid.* **37**, 31 (1988).  
<sup>13</sup>M. Schlüter, James R. Chelikowsky, Steven G. Louie, and Marvin L. Cohen, Phys. Rev. B **12**, 4200 (1975); J. R. Chelikowsky and M. L. Cohen, *ibid.* **10**, 5095 (1974).  
<sup>14</sup>N. W. Ashcroft, Phys. Lett. **23**, 48 (1966).  
<sup>15</sup>M. P. Teter, M. C. Payne, and D. C. Allan, Phys. Rev. B **40**, 12 255 (1989).  
<sup>16</sup>M. Levy, J. P. Perdew, and V. Sahni, Phys. Rev. A **30**, 2745 (1984).  
<sup>17</sup>M. L. Plumer and M. J. Stott, J. Phys. C **18**, 4143 (1985).  
<sup>18</sup>M. Levy and J. P. Perdew, Phys. Rev. A **32**, 2010 (1985).  
<sup>19</sup>N. H. March and A. M. Murray, Proc. R. Soc. London Ser. A **261**, 119 (1961).  
<sup>20</sup>S. Lundqvist and N. H. March, *Theory of the Inhomogeneous Electron Gas* (Plenum, New York, 1983), p. 36.  
<sup>21</sup>R. Car and M. Parrinello, Phys. Rev. Lett. **55**, 2471 (1985).  
<sup>22</sup>J. S. Kasper and S. M. Richards, Acta Crystallogr. **17**, 752 (1964).  
<sup>23</sup>M. T. Yin and Marvin L. Cohen, Phys. Rev. B **26**, 5668 (1982).  
<sup>24</sup>L. W. Wang, Ph.D thesis, Cornell University, 1991.